Strain-based method for assessment of global resistance safety factors for NLNAs of reinforced concrete structures

Engineering Structures 304 (2024) 117625

Contents lists available at ScienceDirect

Engineering Structures

journal homepage: www.elsevier.com/locate/engstruct

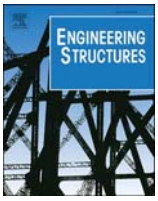

Strain-based method for assessment of global resistance safety factors for NLNAs of reinforced concrete structures

Diego Gino [a], Elena Miceli [a,*], Paolo Castaldo [a], Antonino Recupero [b], Giuseppe Mancini [a,c]

[a] Department of Structural, Geotechnical and Building Engineering (DISEG), Politecnico di Torino, Turin, Italy
[b] Department of Engineering, Università di Messina, Messina, Italy
[c] Engineering Department at SACERTIS Ingegneria s.r.l., Turin, Italy

ARTICLE INFO

Keywords:
Non-linear numerical analysis
Material uncertainty
Peak strain
Global structural resistance
Global safety factors
Reinforced concrete
Safety format

ABSTRACT

This study introduces a novel methodology based on the Global Resistance Format (GRF) for evaluating the design value of the global structural resistance of reinforced concrete (RC) structures. To this aim, an experimental benchmark consisting of 16 RC structural members from the literature has been compiled and the experiments are numerically reproduced through validated non-linear numerical (NLN) modeling assumptions. The tests encompassed various combinations of structural parameters and responses, ranging from brittle to ductile failure modes. The NLN models are used to perform comprehensive probabilistic analyses of the global structural resistance, considering the mechanical uncertainties, to characterize the statistics of the corresponding probabilistic distribution. Then, these statistics have been correlated with the peak strain observed in the primary reinforcement involved in failure mechanism. The peak strain serves as a response indicator representative of the structural failure mode to assess the global safety. The mentioned above correlation allowed to derive predictive expressions that provide the statistical parameters of the global structural resistance as a function of the peak strain in the primary reinforcement. This latter one is computed through a single NLN analysis performed with the mean values of mechanical properties and nominal geometrical ones. In this way, the statistics, so far estimated, can be directly employed to determine the design value of the global structural resistance according to the target reliability levels for both new and existing RC structures. Finally, the achieved results have been compared with those of other established safety formats within the GRF confirming the effectiveness of the proposals.

1. Introduction

Non-linear numerical analyses (NLNAs) of reinforced concrete (RC) structures have become increasingly essential tools for engineers in safety assessment of both new and existing buildings [1–5]. NLNAs, when implemented with solution strategies characterized by appropriate modeling assumptions [6,7], offer a comprehensive understanding of structural responses, even for members with complex boundaries, geometries and loading configurations and/or subjected to degradation phenomena such as reinforcement corrosion [8–11]. Moreover, the adoption of NLNAs by the finite element method allows to perform accurate reliability investigations concerning the dependence of the structural response on the main involved random variables in terms of both aleatory (i.e., actions, geometry and materials properties) and epistemic (i.e., choice of the modeling assumptions - solution strategy, statistics) uncertainties [12–14]. For instance, in order to use the results of NLNAs for safety evaluations in common practice, all the outcomes from NLNAs should be processed including reliability concepts [15,16] accounting for both the aleatory and epistemic uncertainties [14].

In this framework, researchers have invested substantial efforts in establishing standards and safety formats suitable for practical applications of NLNAs on RC structures accounting for the aforementioned relevant uncertainties [15–20]. Moreover, the next generation of international design codes (e.g., Eurocodes gen. 2.0 [21]) will introduce the possibility to adopt such refined approaches for structural verifications. Thus, efficient and easy-to-use methods for reliability analysis through NLNAs are strongly needed. The Global Resistance Format (GRF) [15] is acknowledged as the most efficient method for integrating reliability criteria into safety verifications when NLNAs are adopted. Basically, the GRF grounds on the comparison between the design value of the global structural resistance R_d and the design value of the actions F_d in the considered load combination [15], bypassing cross-sectional

* Corresponding author.
E-mail address: elena.miceli@polito.it (E. Miceli).

https://doi.org/10.1016/j.engstruct.2024.117625
Received 11 October 2023; Received in revised form 23 January 2024; Accepted 4 February 2024
Available online 15 February 2024

verifications and focusing on the global response of the structure. The value of R_d can be estimated by means of NLNAs within the methodology specified by the adopted safety format [15]. The safety formats for NLNAs allow, in principle, to determine R_d according to the target reliability levels related to both new or existing RC structures [15,22].

Despite the notable advantages, the adoption of NLNAs for safety evaluations comes with significant computational demands, resulting in extended processing times and higher associated costs compared to other approaches [23–26]. In fact, the whole process involves three main stages: i). characterization of input variables and model definition; ii). structural analysis; iii). post-processing of the results. The step i) concerns the collection of the available information and knowledge about the structure (different in case of new or existing one), the adoption of the representative values of mechanical and geometrical properties (i.e., mean, characteristic, design or nominal values) [14] and the definition of the solution strategy by means of modeling assumptions (i.e., iterative solution methods to determine equilibrium, kinematic compatibility of displacements and choice of constitutive models) [6] together with its validation for the specific problem. The step ii) relates to structural analysis itself whereas the last one, iii), concerns the understanding of the outcomes of NLNAs. In detail, the analyst should be able to discern between "pure" and "physical" numerical failure of the iterative solution procedure (i.e., not satisfaction of convergence criteria [27–29]). This operation can be particularly complex, especially, if no information about the actual behavior of the structural member at failure is known "a priori" together with the identification of the actual failure mode. According to [30], the failure mode is univocally characterized by the attainment of the ultimate strain of concrete and/or reinforcement in specific locations within the structural member giving rise to global mechanism. Therefore, the achieved material strains in concomitance of the global failure mode can be considered as clear identifiers characterizing the response [30]. However, as demonstrated by [30] and furtherly investigated by [31], the failure mode recognized by means of NLNA can be significantly sensitive to the combination of the representative values of material properties adopted to run the simulation. Depending on the analyzed structure, this issue may give rise to multiple failure modes within, for example, the probabilistic set of NLNAs. For instance, the contribution of multiple failure modes to the overall reliability of a RC structure has been discussed in [30,31]. Specifically, the "non-decreasing assumption" of the response surface of the global structural resistance evaluated as a function of the relevant random variables has been introduced in [31]. In this case, the study [30] highlighted the failure of the commonly adopted safety formats based on the GRF [15] (excluding the pure probabilistic approach) in the estimation of the structural reliability. This further uncertainty has been discussed and covered by means of the request to perform preliminary NLNAs to explore the truthfulness of "non-decreasing assumption" [30,31] for the considered RC structure. If necessary, the value of R_d evaluated with the safety formats based on the GRF (excluding probabilistic methods) [15] should be reduced by an additional factor (denoted also as failure mode-based safety factor) equal to 1.15 [30,31].

Considering these complexities, from model definition to final reliability assessment, the entire procedure to use NLNAs for practical purposes require to have multiple skills for the analyst. Therefore, simplified procedures able to lead to safe reliability evaluations are needed and welcome to promote to practitioners the adoption of NLNAs as a tool for accurate structural verifications also, for example, regarding applications combined with structural health monitoring of existing structures and infrastructures [32–35].

In this context, this study introduces a novel simplified methodology, strain-based approach, within the Global Resistance Format (GRF) for assessing the design value of the global structural resistance R_d. Initially, an experimental benchmark consisting of 16 RC structural members with documented test results from the literature has been compiled and these experiments are numerically reproduced through validated NLN modeling assumptions. The tests included various combinations of structural parameters and responses, ranging from brittle to ductile failure modes. The established NLN models are used to perform comprehensive probabilistic analyses of the global structural resistance, considering the mechanical uncertainties, to characterize the statistics of the corresponding probabilistic distribution. Then, these statistical parameters have been correlated with the peak strain observed in the primary reinforcement at failure. The latter, related to the ultimate limit state condition [18], serves as the relevant response indicator of the failure mode of the structure to assess the global safety. This value is achieved through only one NLNA based on the mean values of material properties and nominal geometrical values. The mentioned above correlation allowed to derive predictive expressions that provide the statistical parameters, related to the mechanical uncertainties, of the global structural resistance as a function of the peak strain in the primary reinforcement. In this way, the statistical parameters, so far estimated, can be directly employed to determine the design value of the global structural resistance according to the target reliability levels for both new and existing RC structures. Finally, the achieved predictions have been compared with those obtained through other established safety formats within the GRF (i.e., Estimation of Coefficient of Variation - ECoV and the Partial Factor Method - PFM [15]) confirming the effectiveness of the proposals.

2. Fundamentals of the global resistance format (GRF) for NLNAs of RC structures

The ultimate limit state verification according to the GRF [15] can be performed comparing the design value of the global structural resistance R_d with the design value of the actions F_d. The global structural resistance is considered as the ultimate global response of the system to the simultaneously insistent set of actions (i.e., within the relevant combination [36]). The limit state condition, according to the GRF [15], can be formulated as follows:

$$F_d \leq R_d \quad where \quad R_d = \frac{R_{NLNA}\left(f_{rep}; a_{rep}\right)}{\gamma_R \cdot \gamma_{Rd}} \tag{1}$$

In Eq.(1), F_d is the design value of the actions; R_d is the design value of global structural resistance against the actions; R_{NLNA} represents the global structural resistance estimated through NLNAs; f_{rep} and a_{rep} are, respectively, the representative values of materials and geometric properties adopted in the NLNAs [14]. The term γ_R denotes the global resistance safety factor related to the uncertainties of material properties and geometry (i.e., aleatory uncertainties) [14,15,30]. The global resistance safety factor γ_R can be determined according to Eq.(2) within the assumption of a lognormal probabilistic distribution for the global structural resistance [14,15]:

$$\gamma_R = \frac{\exp(\alpha_R \beta_t \cdot V_R)}{\delta_R} \geq 1.00 \quad with \quad V_R \leq 0.3 \tag{2}$$

where β_t is the target reliability index [15–22]; α_R is the first order reliability method sensitivity factor assumed equal to 0.8 in the hypothesis of dominating aleatory uncertainties [15,37] with respect to the epistemic ones. The term δ_R groups the influence related to the bias factors of geometrical properties deviations $\delta_{R,g}$ and to the *mean-to-mean* deviation $\delta_{R,m}$ [14,31], as explained in the following, and can be computed as:

$$\delta_R = \delta_{R,m} \cdot \delta_{R,g} \tag{3}$$

The latter one quantifies the discrepancy between the result from one NLNA performed with mean values of material properties and nominal values for geometrical characteristics with respect to mean value of the global structural resistance given by a probabilistic analysis [14,17]. As for $\delta_{R,g}$, it can be set equal to 1 for general cases excluding strongly slender systems [14].

The term V_R of Eq.(2) represents the coefficient of variation (CoV) of

the global structural resistance (assumed as log-normally distributed variable), inclusive of the influence of aleatory uncertainties related to both materials and geometrical properties [14]. This value can be estimated according to Eq.(4) (within an error of 5%):

$$V_R = \sqrt{V_{R,m}^2 + V_{R,g}^2} \quad with \quad V_R \leq 0.3 \tag{4}$$

where, $V_{R,m}$ represents the CoV of the global structural resistance associated to the aleatory uncertainty of material properties while, $V_{R,g}$ denotes the CoV related to the aleatory uncertainty of geometrical properties. The value of $V_{R,g}$ has been studied by [14], and for non-slender RC structural elements, it can be considered reasonably equal to 0.05, also in line with [15].

Regarding the value of $V_{R,m}$ or the direct evaluation of R_d in Eq.(1), the following safety formats within the GRF [15] together with the probabilistic method have been proposed:

1. *Partial Factor Method (PFM)* [15,31]: this safety format allows to carry out the safety verification performing 1 NLNA using the design values as representative ones of materials and geometrical properties (i.e., f_d and a_d, respectively). The design values of material properties should be derived in line with the specifications of [15,18,22] and deprived of the contribution of the model uncertainty for standard verifications [21]. This may lead to complexities, especially, when existing RC structures are considered [22]. Eq.(1) applies using f_d and a_d as representative values, setting γ_R as unit and adopting the appropriate value for γ_{Rd}.
2. *Global Resistance Method (GRM)* [15]: this safety format adopts, as representative values of materials and geometrical properties, the mean values f_m and nominal ones a_n, respectively. The value of γ_R can be estimated in line with Eq.s(2)-(4) whereas, γ_{Rd} should be determined as needed. In particular, the value of the CoV $V_{R,m}$ can be determined according to:

   i. *standard Estimation of Coefficient of Variation Method (ECoV)* [19] with the assumption of lognormal distribution for the global structural resistance and performing two NLNAs with, respectively, mean/nominal (i.e., f_m and a_n) and characteristic/nominal (i.e., f_k and a_n) values concerning the representative values of materials/geometrical properties [15].
   ii. *probabilistic evaluation of coefficient of variation* [15,21] with the probabilistic analysis of the global structural resistance characterizing $V_{R,m}$ including aleatory uncertainties related to material properties.

3. *Probabilistic method (PM)* [15]: this safety format investigates the structural resistance accounting for aleatory and epistemic uncertainties as random variables and directly deriving the design value of the global resistance R_d as a function of the expected target reliability level.

The term γ_{Rd} of Eq.(1) denotes the model uncertainty safety factor and accounts for the epistemic uncertainties in NLNAs [38–43] related to choices made by the analyst in defining the numerical model. These choices concern all the assumptions referred to equilibrium evaluation, kinematic compatibility of displacements and constitutive laws for materials [38–43]. Several studies have been carried out giving an exhaustive characterization of this coefficient concerning quasi-static monotonic and cyclic loads, slender members, 2D and 3D NLNAs [38–43]. In detail, [38–43] propose fixed values of γ_{Rd} which are safely conceived to cover both "between" (different solution strategies used to analyse one RC member) and "within" (one solution strategy used to analyse different RC members) model uncertainty [43] accounting for the various suitable solution strategies available to different analysts [41]. It is important to emphasize that the calibration of the global safety factors γ_R and γ_{Rd} is entirely independent as they related to uncertainties of different nature (i.e., aleatory and epistemic) [38]. The adoption of the value of γ_{Rd} should be always performed according to the same target reliability index β_t used for the evaluation of γ_R.

Finally, Eq.(1) can be modified, if necessary, to take into account the multiple failure modes in case of not compliance to "non-decreasing assumption" [30,31] by means of an additional factor equal to 1.15. In next section, the outline of the proposed novel methodology (i.e, strain-based approach) within the GRF to estimate the design value of the global structural resistance is presented.

3. Outline of the novel strain-based methodology to assess the global resistance safety factors γ_R for NLNAs of RC structures

This section describes the philosophy of the strain-based methodology devoted to estimate the global resistance safety factor γ_R for safety verifications of RC systems using NLNAs. The proposed methodology can be contextualized as a novel approach to estimate the CoV of the global resistance related to aleatory uncertainty associated to material properties $V_{R,m}$ within the safety format denoted as Global Resistance Method (GRM) according to the general GRF, as described in Section 2.

The calibration philosophy is summarized in Fig. 1. First, an experimental benchmark was established, comprising 16 RC structural components with thoroughly documented test results from the literature [44–47]. These tests covered a range of different material properties and structural responses, encompassing both brittle and ductile failure modes with the aim to propose a comprehensive methodology to assess R_d. Subsequently, a series of modeling assumptions has been devised to reduce model uncertainty [42], leading to 16 NLN models suitable for conducting a set of probabilistic analyses of the global structural resistance. Probabilistic models for the relevant aleatory uncertainties have been defined according to [48] and accounting for differentiation between basic assumptions about statistical parameters of material properties, with particular care to concrete quality.

In fact, according to [15], with reference to new RC structural members, the CoV of the concrete cylinder compressive strength V_c can be assumed, on the safe side, equal to 0.15. However, this value is very sensitive to the quality of the concrete casting and construction technology with particular reference to existing systems [49–52]. For instance, to propose a methodology suitable for new and existing structures with different ages, three different CoV values for the concrete cylinder compressive strength V_c have been assumed and set to 0.15, 0.20 and 0.25, respectively. The probabilistic analyses have been carried out adopting the Latin Hypercube Sampling (LHS) method [53] with 30 samples [19,30] to approximate the random response of each one of the 16 RC structural members and for each one of the 3 CoV V_c. This has led to an extensive campaign composed of 1440 NLNAs with a relevant computational time. The results of these probabilistic analyses enable to characterize the probability distribution of the global structural resistance with the related statistical parameters (i.e., mean value $\mu_{R,m}$ and CoV $V_{R,m}$ [14]) for each one of the selected 16 RC members [44–47].

The statistical parameters, that have been estimated thus far considering the materials uncertainty, can be correlated to the significant peak strain $\varepsilon_{s,max}$ observed in the primary reinforcement in the failure mechanism. In this investigation, the term "primary reinforcement" denotes the tensile reinforcement bars involved within the global resistance mechanism (i.e., failure mode). This relevant response indicator can be achieved as result of a single NLNA, conducted using the mean values f_m as representative ones for material properties and adopting nominal values a_n for geometrical properties (Fig. 2). The correlation between the statistical parameters related to global structural resistance and the peak strain allows for the derivation of predictive expressions (Fig. 2) to compute the CoV of the global structural resistance $V_{R,m}$ depending only on $\varepsilon_{s,max}$. In this way, it is possible to calculate the design value R_d according to the safety format GRM [15], aligning it with the desired reliability levels for both new and existing RC structures (Fig. 2).

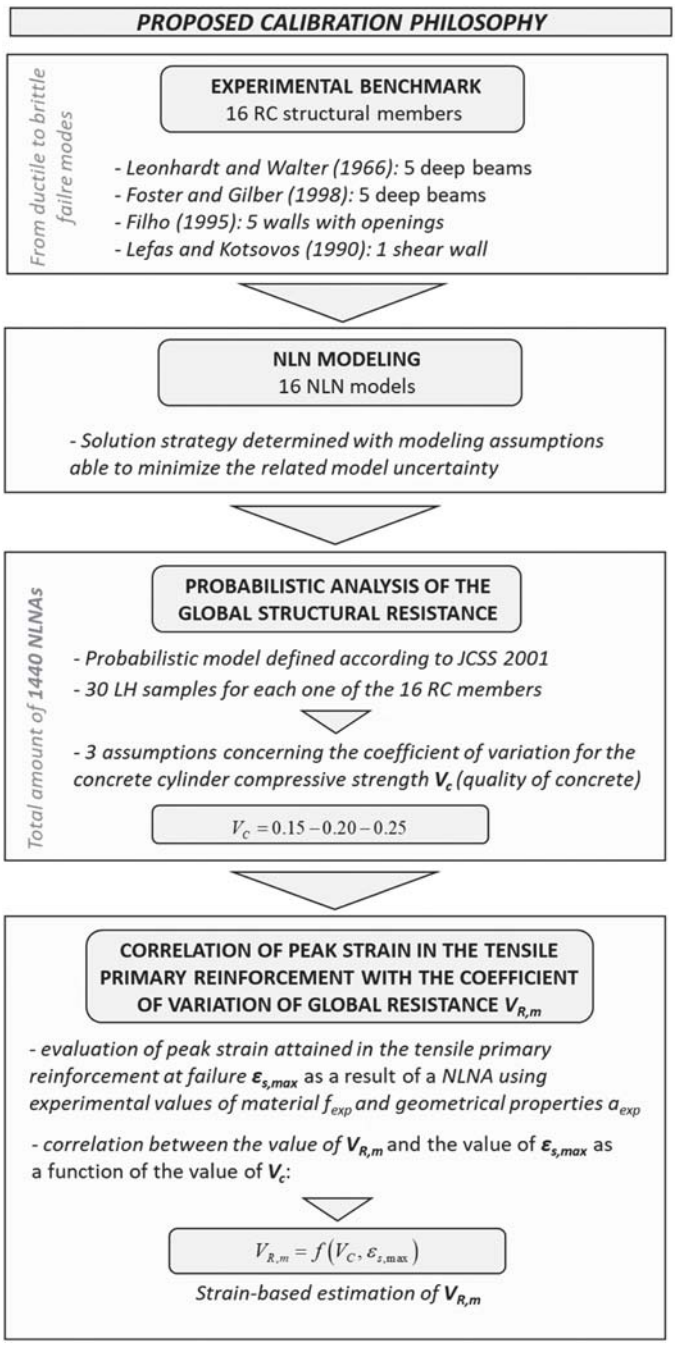

Fig. 1. Proposed calibration philosophy for the novel strain-based approach to estimate the CoV $V_{R,m}$.

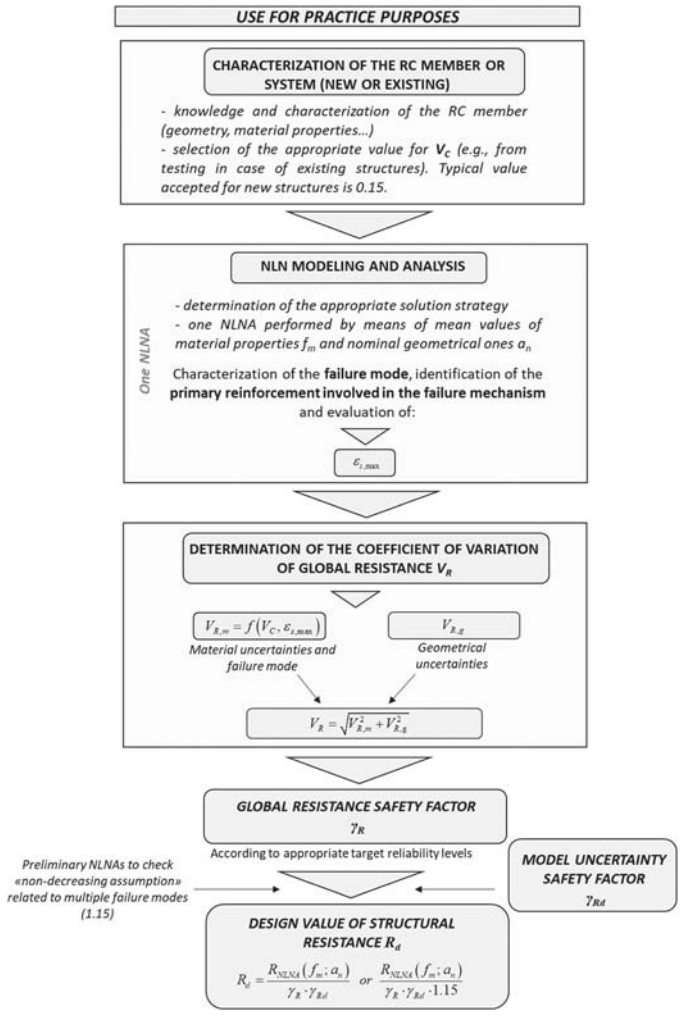

Fig. 2. Proposed calibration philosophy for the novel strain-based approach to assess R_d.

In the next, the description of the selected 16 RC members [44–47] is reported together with the results useful to the implementation of the novel strain-based methodology.

4. Experimental benchmark and numerical modeling

In this section, the 16 RC members selected to implement the proposed methodology are presented in their main characteristics [44–47]. Then, the solution strategies [6] and related modeling assumptions to perform NLNAs are outlined and validated.

4.1. Experimental tests benchmark

This subsection introduces the set of experimental tests selected to be reproduced by means of NLNAs and adopted to perform the probabilistic investigation of the global structural resistance considering the materials uncertainty. The selection has been carried out to achieve a well-balanced range of material properties that encompass the limits of applicability specified in current design codes [15,18], and to cover the transition from brittle (i.e., concrete failure without yielding of the primary reinforcement) to ductile (i.e., concrete failure with yielding of the primary reinforcement) failure modes. In detail, an experimental set composed of 16 RC structural members realized and tested by [44–47] is considered. All the selected RC members have been realized with isostatic restraint scheme configuration and loaded through appropriate apparatus according to the descriptions detailed in [44–47].

In [44], the experimental results achieved by Leonhardt and Walther are described. They have analysed five deep beams denoted respectively as WT2, WT3, WT4, WT6 and WT7. All these deep beams were 1.6 m wide and 1.6 m high with a uniform thickness of 0.10 m. The reinforcement is composed of both horizontal and vertical stirrups, along with additional bars located in the lower part of the structural elements. The concrete cylinder compressive strength varies between 26.7 and 28.7 MPa in the different tests, while the mechanical properties of the reinforcement are determined by the diameter of the bars used. WT2, WT3 and WT4 walls are subjected to top-down loading and differ in terms of the amount of reinforcement in their lower sections. The horizontal and vertical stirrups have a diameter of 5 mm and are spaced at 26 mm intervals. In Fig. 3(a), the schematic representation of the deep beam WT2 is reported in the *"Scheme a"* arrangement. WT2 specimen

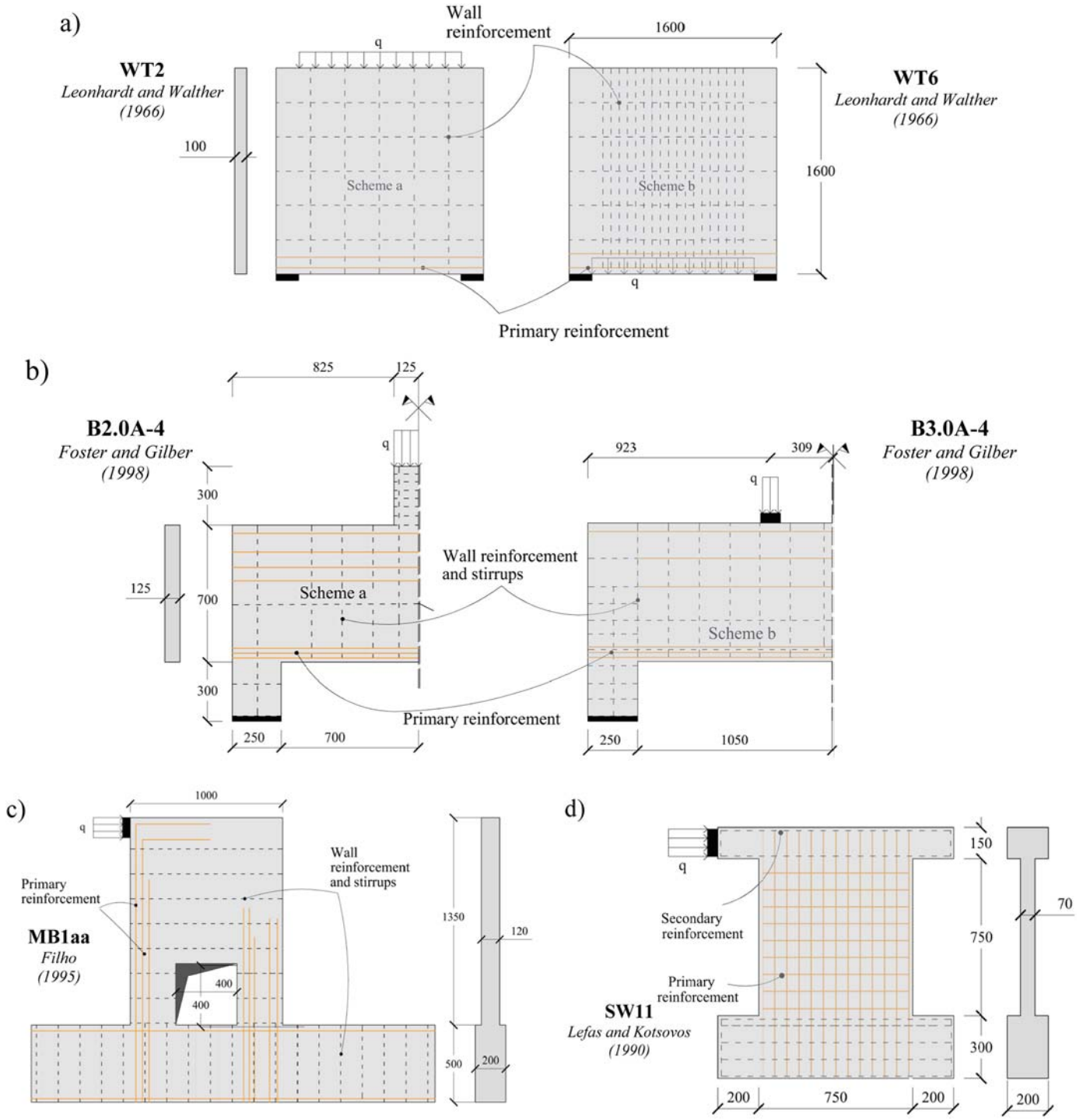

Fig. 3. Schematic representation of some RC members tested by [44–47]. Measures in millimeters.

failed due to the yielding of longitudinal bars at the midspan with formation of large vertical cracks, whereas WT3 failed due to concrete crushing at the supports before the yielding of reinforcement with vertical cracks at the level of bottom chord. Additionally, the specimen "WT4″ failed due to concrete crushing at the side enlargement of the cross section with longitudinal bars yielding and sub-vertical cracking development within the wall. WT6 and WT7 structures, which vary in terms of both the distribution of applied loads and reinforcement, are loaded from the bottom as shown in Fig. 3(a) concerning WT6 member (*Scheme b*). For both WT6 and WT7 specimens, the experimentally observed failure modes involved the yielding of the main longitudinal reinforcement with concrete crushing at the edge supports. The cracking exhibited a characteristic "arched-shaped" path typical of the deformation induced by suspended loads.

The experimental findings discussed by Foster and Gilbert in [45] pertain to five RC deep beams, each measuring 0.7 m in depth and 0.125 m in thickness. These beams are designated as B2.0–1, B2.0–3, B3.0–1, B2.0A-4 and B3.0A-4. Beams denoted as B2.0–1, B2.0–3 and B3.0–1 (*Scheme a*) differ from B2.0A-4 and B3.0A-4 (*Scheme b*) beams in terms of their load arrangements. Fig. 3(b) shows the two different schemes reporting, as an example, the deep beams defined as B2.0A-4 and B3.0A-4. The primary tensile reinforcement consists of six

20 mm-diameter longitudinal bars. Web reinforcement comprises 6.3 mm-diameter bars spaced at 75 mm intervals in the transverse direction and 6.3 mm-diameter bars spaced at 135 mm intervals in the longitudinal direction. The compressive concrete strength varies within the range from 78 to 88 MPa across the different tests. B2.0–1, B2.0–3, B3.0–1 and B3.0A-4 deep beams exhibited failure with concrete crushing at the edge of the loading column after the yielding of the longitudinal reinforcement in the bottom chord. This was accompanied by flexural cracks significantly wider than the diagonal cracks. On the other hand, B2.0A-4 specimen demonstrated concrete crushing in the main body of the wall with opened diagonal cracks and longitudinal reinforcement yielding.

Filho [46] conducted experimental tests on five RC walls with openings, labeled as MB1aa, MB1ae, MB1ee, MB1ee1 and MB4ee. These walls share the following geometrical properties: they are 1.35 m high, 1 m wide, 0.12 m thick and they are supported by a lower foundation beam that is 0.2 m thick and 0.5 m high. These structures feature a square opening that is 0.4 m wide, fully constrained at the base, and are subjected to horizontal loading at the top. The concrete cylinder compressive strength varies from 39 to 42 MPa in the different tests while, the amount of reinforcement varies significantly between the structures, although the general layout of the main reinforcements remains consistent. Fig. 3(c) shows the schematic representation of the test "MB1aa". Regarding the experimental failure modes of these walls, all the specimens exhibited a brittle or nearly brittle response with the formation of an inclined compression strut starting from the loading plate to the edge of the opposite column, coinciding with concrete crushing at the connection to the stiff foundation.

The experimental findings examined by Lefas and Kotsovos [47] center around a RC wall identified as SW11. This wall measures 1.2 m in height, 0.75 m in width, 0.07 m in thickness, and it is reinforced by upper and lower beams, each 0.2 m thick. The structural member is fully anchored at its base and subjected to horizontal loading at the top. The concrete has a compressive strength of 43 MPa and the reinforcement consists of horizontal bars with 6.25 mm-diameter bars spaced at 80 mm and vertical bars with 8 mm-diameter bars spaced at 60 mm. The experimentally observed failure mode consisted of the development of inclined cracks within the wall, accompanied by concrete crushing at the compressed edge with reinforcement yielding on the opposite tensile side.

4.2. Solution strategy and NLNAs results

This subsection describes the modeling assumptions [6,40–42] employed to create the NLN models for the previously described 16 RC structural elements. The "*ATENA 2D*" software platform [54] has been used for this purpose. The body of 16 RC members has been represented by quadrilateral plane stress finite elements, denoted as CCQ10SBeta [54], featuring quadratic displacement interpolation functions [54]. The finite element mesh size has been established following a calibration process for each structural element, ranging between 5 cm and 10 cm with the aim to meet both accuracy in terms of predictions of the experimental outcomes and computing expenses. The solution of nonlinear system of equations has been accomplished using the standard Newton-Raphson iterative approach [27], with a maximum iteration limit set at 200 and convergence criteria based on forces and energy, with tolerances set at 1% and 0.01%, respectively.

As for the constitutive models, the non-linear behavior of concrete under compression and tension has been replicated using the "*SBeta material model*" available within the platform "*ATENA 2D*" [54]. Concerning the mono-axial concrete response, the "*SBeta material model*" incorporates curvilinear response in compression with post-peak response with linear compression softening (LCS). The concrete tensile behavior is elastic until tensile strength is reached with post-peak behavior according to linear tension softening (LTS). The LCS law has been calibrated in a manner that ensures, after that the peak load and related strain have been reached, a 50% reduction in compressive strength in concomitance of the ultimate compressive strain of concrete [55]. Instead, the LTS law has been appropriately calibrated for each structural member in such a way to optimize the prediction in comparison to the experimental one [38]. In detail, the ultimate strain in tension has been set between 2 and 10 times the tensile strain corresponding to tensile strength of concrete [38] with the aim to account for fracture energy. As for cracking behavior, the smeared crack modeling approach has been used, with the rotated crack model [54]. It can simulate the progressive development and rotation of cracks within the concrete as load is applied, accurately capturing post-cracking behavior. Concrete properties have been assigned according to the experimental data available in [44–47]. If data are not available from the original scientific studies [44–47], any missing parameter has been adopted according to [18].

Regarding the reinforcement, a bilinear constitutive law with hardening rule has been employed to simulate the behavior of steel in both compression and tension. The key properties have been determined in accordance with the experimental findings [44–47]. The Young's modulus of the steel reinforcement has been assumed to be 200 GPa, with an associated ultimate strain ε_u of 9% [14]. The yielding strain ε_y for the reinforcement has been determined based on the previous experimental data and assumptions. The reinforcement has been represented using both smeared (for the wall, shear and secondary reinforcement) and discrete approaches (for the primary reinforcement) [27,54], following the schematic configurations depicted in Figs. 3–7.

The numerical simulations have been conducted following the experimental loading procedure, initially, applying the dead load, and then incrementally applying the experimental actions until failure occurred. The size of the load steps has been defined with the aim to have a good degree of accuracy and acceptable computational cost. The displacements monitored within the numerical simulations correspond to those indicated in Figs. 4–7.

Additionally, the peak strains reached within the primary reinforcement at the point of failure $\varepsilon_{s,max}$ have been recorded for each NLNA. The failure of the NL iterative solution procedure occurs in the last load step which fuls the adopted convergence criteria. Care has been devised to characterize the failure mechanisms to avoid "pure" numerical failures and meet "physical" ones in line with the experimental tests. Similar attention has been performed concerning each one of the 1440 NLNAs needed for the probabilistic investigation discussed in the next section.

Figs. 4–7 show the results from the NLNAs performed using the experimental values of both materials (f_{exp}) and geometrical (a_{exp}) properties (i.e., $R_{NLNA}(f_{exp};a_{exp})$) in comparison to the experimental outcomes (R_{exp}). The details of the failure modes recognized by means of NLNAs are also reported together with the experimental properties of both concrete and primary reinforcement. The failure modes and crack patterns observed in the numerical simulations are consistent with the experimental ones as briefly described in Section 4.1 and exhaustively presented by [44–47]. Moreover, the displacements monitored during the NLNAs align with experimental ones depicted in Figs. 4–7. In addition, for each NLNA, Figs. 4–7 also illustrate the position where the peak strain of the primary reinforcement at failure, denoted as $\varepsilon_{s,max}$, is reached and recorded. In cases where the yielding of the primary reinforcement has occurred, the related first yielding point is also reported in Figs. 4–7. Generally, the improved refinement of the various solution approaches has resulted in proper agreement with the experimental results, effectively capturing the actual behavior observed during all the experimental tests.

A more comprehensive assessment of the proposed solution strategies can be achieved by examining the ratio $\vartheta = R_{exp}/R_{NLNA}(f_{exp};a_{exp})$ [15,38–43] with respect to $\varepsilon_{s,max}$. The ϑ value represents, for the chosen solution strategy and the specific RC structural member, the observed realization of the random variable associated with model uncertainty [38–43]. Fig. 8 illustrates the trend of the observed values of ϑ with

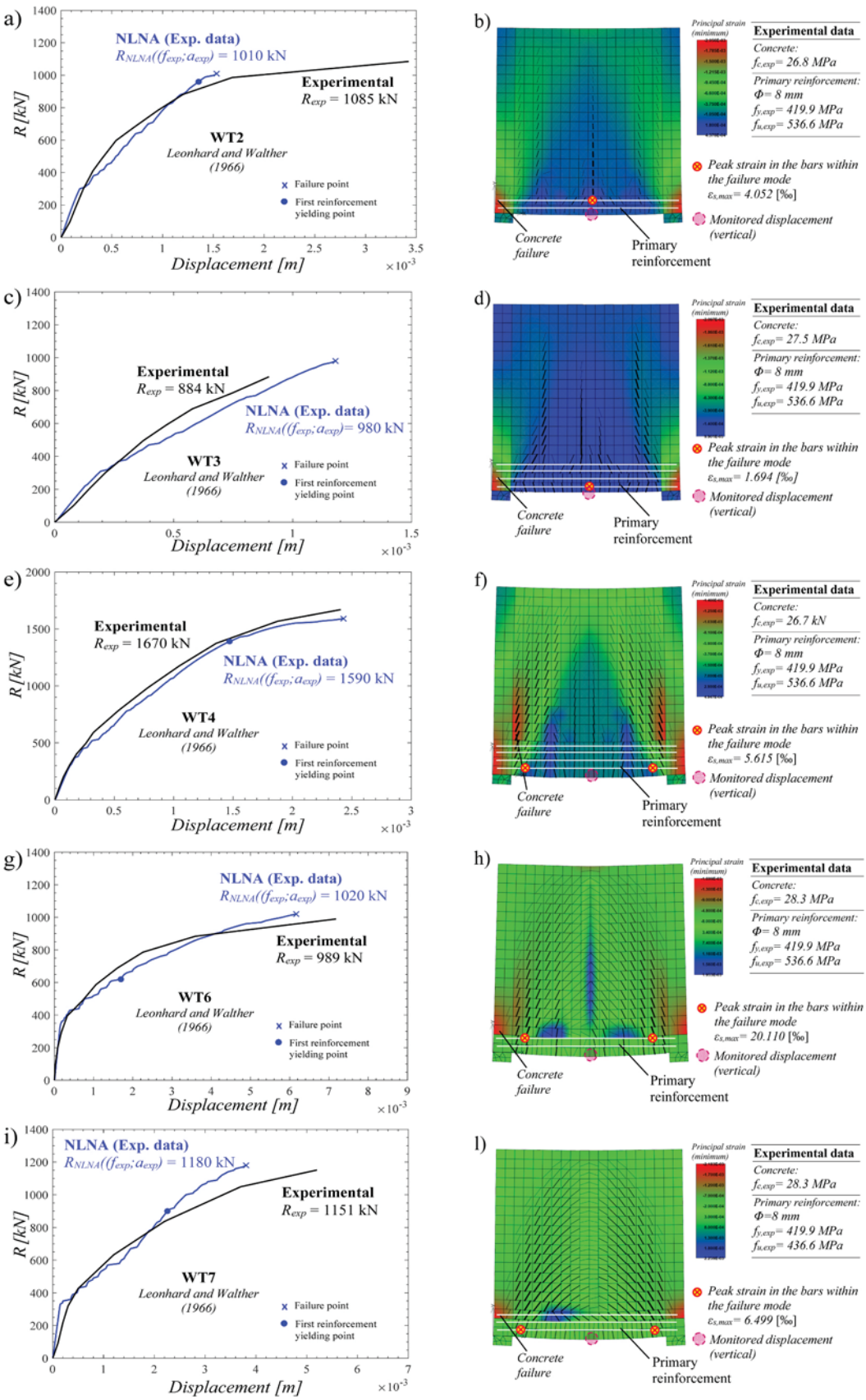

Fig. 4. RC members tested by [44]: comparison between experimental results R_{exp} and NLNAs outcomes $R_{NLNA}(f_{exp};a_{exp})$ (a, c, e, g, i); representation of the failure mechanism in concomitance of failure (b, d, f, h, l).

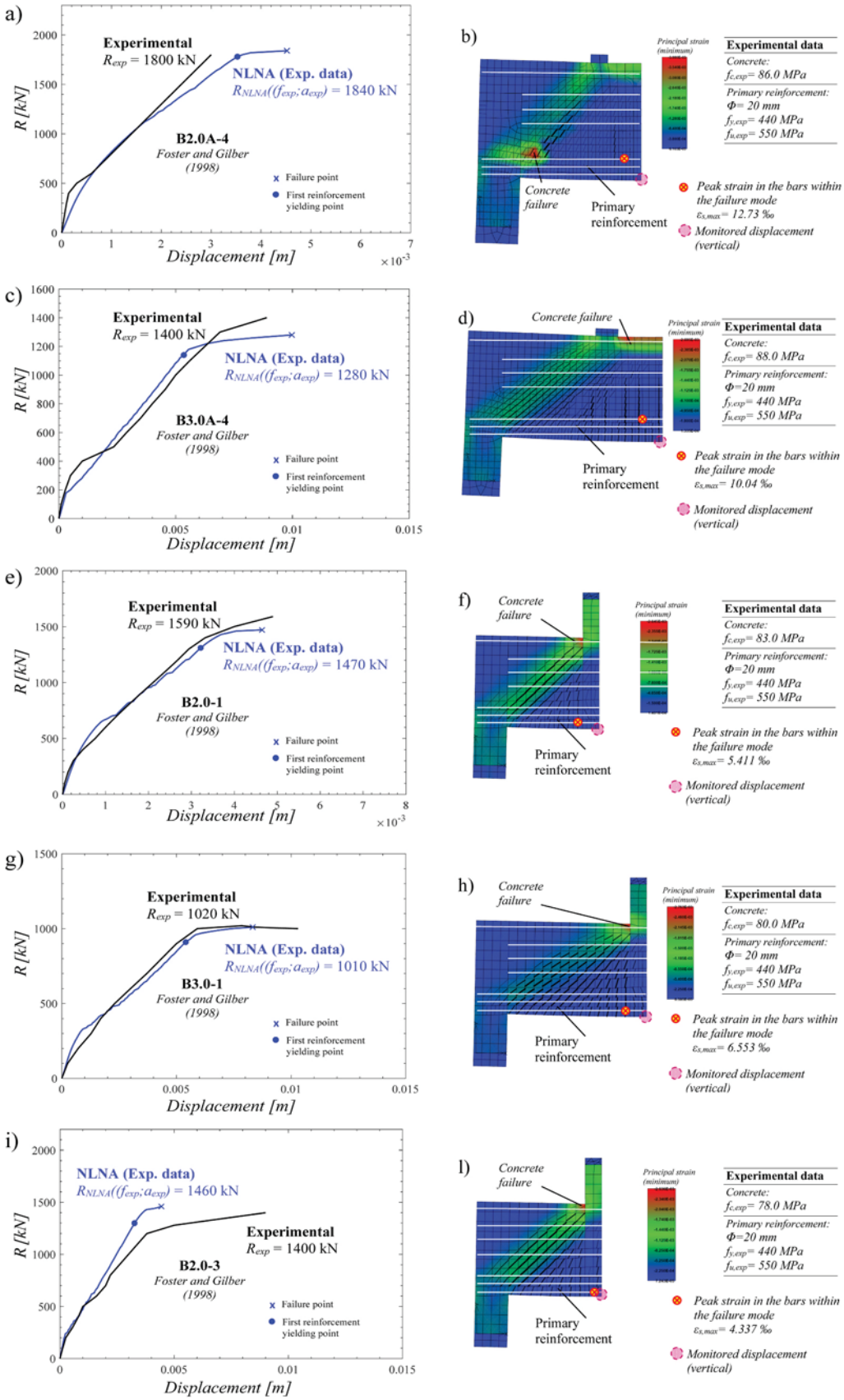

Fig. 5. RC members tested by [45]: comparison between experimental results R_{exp} and NLNAs outcomes $R_{NLNA}(f_{exp};a_{exp})$ (a, c, e, g, i); representation of the failure mechanism in concomitance of failure (b, d, f, h, l).

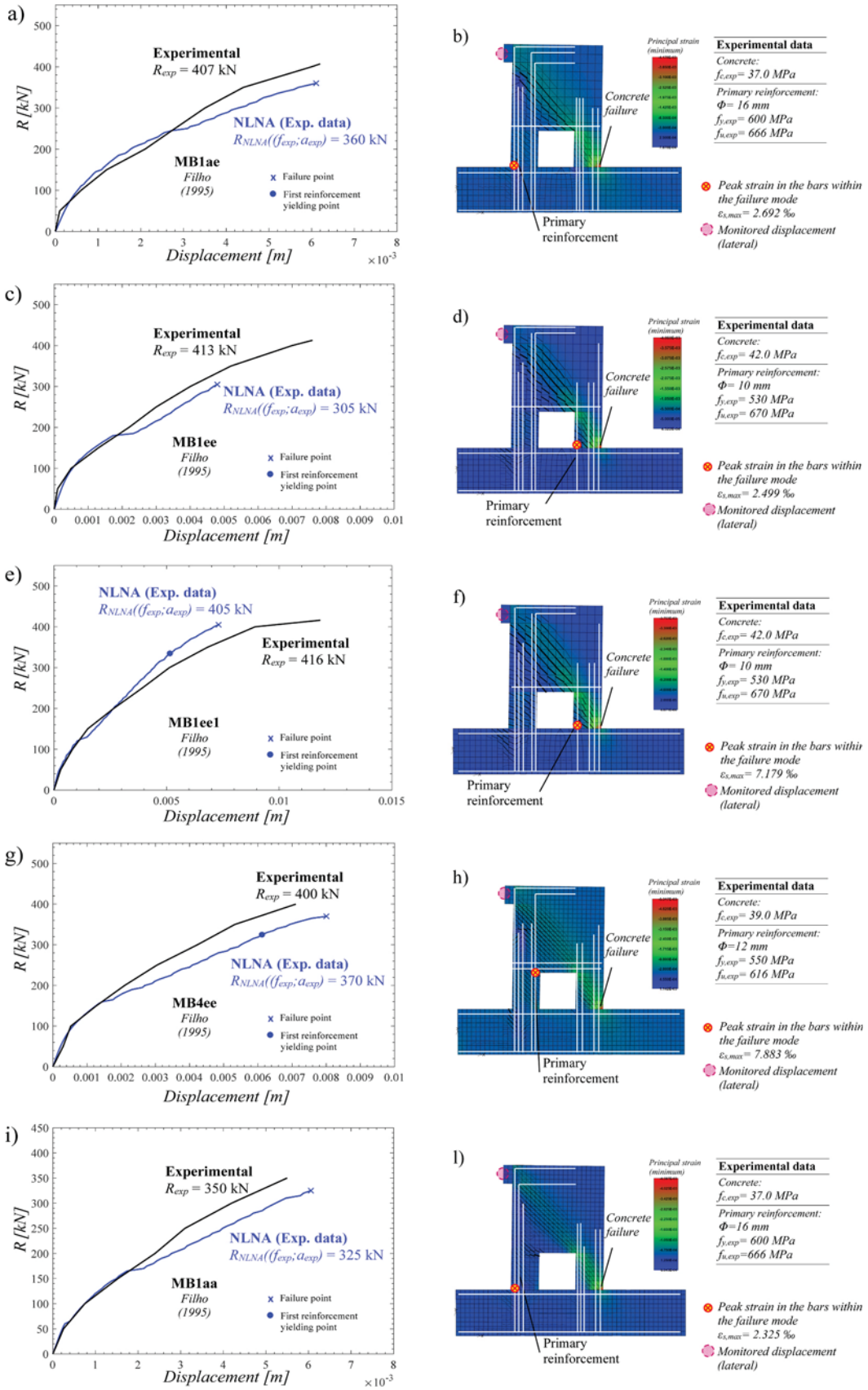

Fig. 6. RC members tested by [46]: comparison between experimental results R_{exp} and NLNAs outcomes $R_{NLNA}(f_{exp};a_{exp})$ (a, c, e, g, i); representation of the failure mechanism in concomitance of failure (b, d, f, h, l).

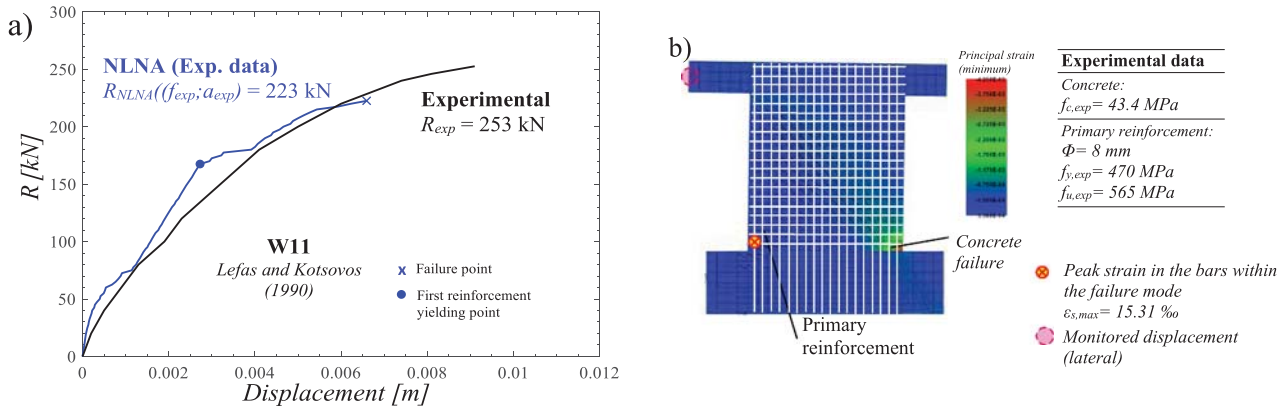

Fig. 7. RC member tested by [47]: comparison between experimental results R_{exp} and NLNAs outcomes $R_{NLNA}(f_{exp};a_{exp})$ (a); representation of the failure mechanism in concomitance of failure (b).

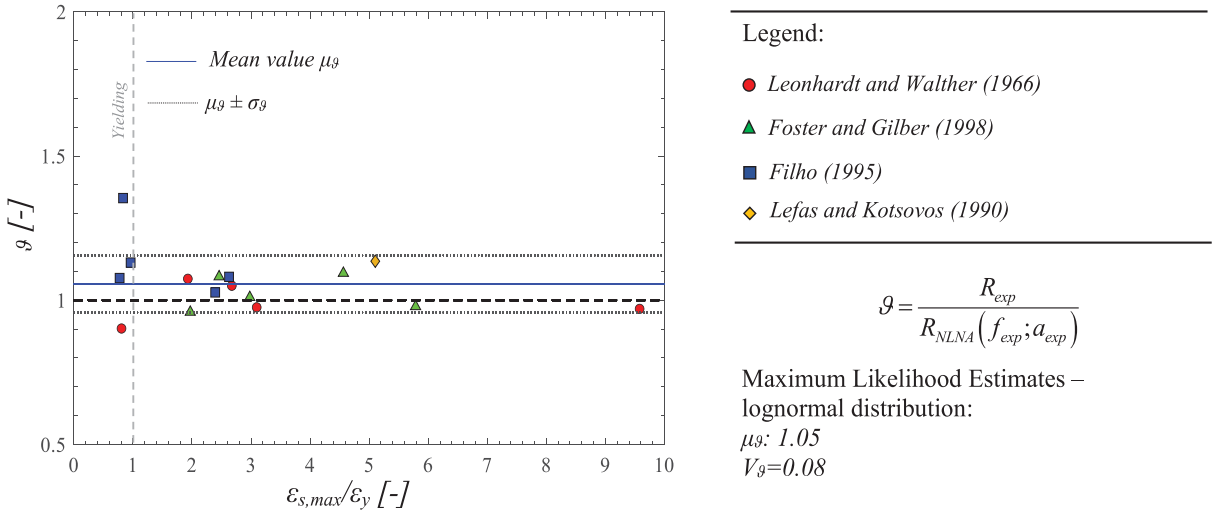

Fig. 8. Representation of the realization of the model uncertainty random variable for the considered solution strategy and RC members [44–47].

respect to the ratio between the peak strain at failure reached in the primary reinforcement in the NLNAs, $\varepsilon_{s,max}$, and the corresponding yielding strain, ε_y. The ϑ data have been statistically characterized using the Maximum Likelihood (ML) method, assuming a lognormal distribution with a mean value μ_ϑ and a CoV V_ϑ [40–43].

According to [42], these values, to be representative of the uncertainty related to the assumptions performed within NLNAs only, should be deprived of the influence of the experimental uncertainty. To do so, the approach of [42] is herein adopted assuming a limited influence of the latter [42,56]. With respect to the adopted solution strategy, it can be observed that for brittle failure mechanisms (i.e., $\varepsilon_{s,max}/\varepsilon_y < 1$), the dispersion of ϑ appears to be larger compared to progressively more ductile responses (i.e., $\varepsilon_{s,max}/\varepsilon_y \geq 1$), although with a safe bias ($\mu_\vartheta > 1$) [40]. The uncertainty related to the assumptions in numerical modeling seems to sightly decrease for increasing values of the ratio $\varepsilon_{s,max}/\varepsilon_y$ approaching unbiased solutions (i.e., $\mu_\vartheta \approx 1$). This result agrees with [39]. Considering all the results, the values of μ_ϑ and V_ϑ are 1.05 (indicating safely biased models) and 0.08, respectively.

Note that, if more solution strategies (i.e., different software codes) had been adopted to solve the same structural problem, a more comprehensive statistical analysis would have been valuable to assess μ_ϑ and V_ϑ depending on the characteristics of the failure modes [38,41–43].

Based also on the results presented by [40–43], it can be concluded that the modeling assumptions used in this study are suitable for conducting a probabilistic investigation of the structural response.

5. Probabilistic characterization of the global structural resistance

This section presents the modeling assumptions adopted for the probabilistic analysis of the structural response, carried out using the LHS method [53] to sample the mechanical uncertainties. Subsequently, the results of this probabilistic analysis are discussed, focusing on the statistical parameters derived for the global structural resistance concerning the 16 RC members [44–47].

5.1. Probabilistic hypotheses for sampling relevant random variables

The sampling technique together with probabilistic hypotheses, herein adopted, are presented in the following. As mentioned above, the LHS [53] method has been used to generate 30 samples. Consistent with prior researches [14,19,30] the sampling size is sufficient, provided that the overall CoV for the involved variables and global response remains below 0.3 (with an error margin within 5% on the statistical parameters estimate).

With reference to the relevant random variables, the adopted probabilistic models adhere to the specifications outlined in JCSS Probabilistic Model Code 2001 [48] including linear correlations among the

correlated random variables.

As the aim of this study is to investigate the influence of aleatory uncertainties related to material properties on the global structural response (i.e., CoV $V_{R,m}$), the probabilistic analysis employs the random variables listed in Table 1. The material properties dependent on any random variable in Table 1 are derived in accordance with [18] (e.g., tensile strength f_{ct} and Young's modulus E_c of concrete) for each sample. In Table 1, the mean values of the relevant random variables are assumed as the experimental ones reported by the original literature for the 16 RC members [44–47]. Therefore, with the term experimental values we will hereafter refer to the mean values of the representative probabilistic distributions of the material properties [14]. The coefficients of variation of material properties are set in Table 1 in agreement with [48]. Specifically, in alignment with the framework provided in Section 3, the CoV V_c for the concrete cylinder compressive strength f_c has been characterized by three different assumptions (i.e., 0.15, 0.20, 0.25) to account for its quality variability [49,50]. Differently, the mechanical properties related to reinforcement steel have been modeled using a single probabilistic approach [15,48]. This choice is justified by the expectation that these properties are less susceptible to quality issues during the construction of RC structures and are sourced from industrial production processes [57].

Regarding the geometrical properties, the experimental values will be considered equivalent to their nominal ones [30].

Subsequently, for each one of the 16 RC members, 30 LH samples of each random variable have been generated for each assumed value of V_c.

5.2. Outcomes from probabilistic analysis of the global structural resistance

In this subsection, the main outcomes from the probabilistic analysis performed with the random variables above introduced are discussed. The LH sampled random variables of Table 1 have been useful to determine 30 × 16×3 NLN models adopting the solution strategy calibrated in Section 4 with reference to the experimental values of both materials and geometrical properties. The load vs displacement curves related to the different sets of the probabilistic investigation are reported in Figs. A1–4 of the Annex A. The results of the NLNAs in terms of global structural resistance R (i.e., load associated to the last step able to fulfill the convergence criteria) are summarized in Figs. 9–12. In detail, Figs. 9–12 show, for each one of the 16 RC members [44–47], the "empirical" and the "best-fitted" Cumulative Density Function (CDF) related to R. The Anderson-Darling statistical tests [60] have been performed on the 30 results of the global structural resistance R for each RC member concerning the three assumptions for the concrete cylinder compressive strength CoV V_c. The Anderson-Darling test has been used to assess whether the mentioned above outcomes follow a lognormal distribution (i.e., null hypothesis). The null hypothesis, that is the assumption of lognormal distribution for the global structural resistance R, has been tested and confirmed at a 5% significance level for each set of sampled NLN models as shown in Figs. 9–12 in terms of high "P-value" values. In this way, the random variable representing the global structural resistance can be described using a lognormal distribution [8,14,15,30], with statistical parameters estimated by means of the ML method [59]. The ML estimates of the statistical parameters lead to the characterization of the mean value $\mu_{R,m}$ and CoV $V_{R,m}$ of the global structural resistance R for each set of the 30 NLNAs. The values of $\mu_{R,m}$ and $V_{R,m}$ are reported in Figs. 9–12 together with the ratio denoted as $\delta_{R,m}$. In line with [14], the value of $\delta_{R,m}$, named "*mean-to-mean deviation*", represents the deviation of the mean value of the global resistance achieved by the probabilistic analysis $\mu_{R,m}$ from the value of the global structural resistance estimated using experimental values of both material and geometrical properties $R_{NLNA}(f_{exp};a_{exp})$ (Section 4). Note that, in this investigation, the experimental values are assimilated to mean values (f_m) and nominal values (a_n), respectively, for mechanical and geometrical properties. For instance and, in general, the *mean-to-mean* deviation $\delta_{R,m}$ can be computed as:

$$\delta_{R,m} = \frac{\mu_{R,m}}{R_{NLNA}(f_{exp};a_n)} = \frac{\mu_{R,m}}{R_{NLNA}(f_m;a_n)} \tag{5}$$

Note that the probabilistic analysis sheds light on the overall structural response and reveals variations in failure modes for the different combinations of material properties as also widely discussed in [30,31]. However, the failure mechanism associated with simulations using experimental material and geometrical properties values (i.e., mean and nominal) emerges as the most likely one.

The computed values of both the *mean-to-mean* deviation $\delta_{R,m}$ and CoV $V_{R,m}$ of the global structural resistance can be expressed as a function of the strain ratio $\varepsilon_{s,max}/\varepsilon_y$ (as disclosed in previous sections). It is important to highlight that, for each RC member, the value of $\varepsilon_{s,max}$ is derived from the NLNA performed using the experimental values of materials and geometric properties (i.e., mean and nominal, respectively) as reported in Figs. 4–7 of Section 4. Concerning the yielding strain ε_y, it is evaluated according to the experimental material properties for each RC member (Section 4). The strain ratio, $\varepsilon_{s,max}/\varepsilon_y$, serves as a straightforward parameter able to monitor the NLNA, providing insights into the structural response and nature of the failure mode, whether it is fully ductile or fully brittle or intermediate. Consequently, this parameter is highly suitable for establishing a general guideline to determine $\delta_{R,m}$ and $V_{R,m}$ for practical applications. Specifically, considering the results associated to the 16 RC members [44–47], the following expressions have been derived with the aim to relate $\delta_{R,m}$ and $V_{R,m}$ to the strain ratio $\varepsilon_{s,max}/\varepsilon_y$:

$$\delta_{R,m} = a \cdot \left(\frac{\varepsilon_{s,\,\max}}{\varepsilon_y}\right) + b \tag{6}$$

$$V_{R,m} = V_c \cdot \left(\frac{\varepsilon_{s,\,\max}}{\varepsilon_y} + 1\right)^{\eta} \quad with \quad V_y \le V_{R,m} \le V_c \tag{7}$$

In Eq.s(6)-(7), the coefficients a, b and the exponent η, have been estimated by means of the least square method [58] with the aim to

Table 1
Characterization of the probabilistic models related to the aleatory uncertainties associated to material properties with reference to the 16 RC members of [44–47].

Random variable	Probabilistic distribution	Mean value	Coefficient of variation [-]	Statistical correlation	Ref.
Concrete cylinder compressive strength f_c [MPa]	*Lognormal*	$f_{c,exp}$	0.15 – 0.20 – 0.25	-	[15, 48]
Reinforcement tensile yielding strength f_y [MPa]	*Lognormal*	$f_{y,exp}$	0.05	f_u (0.85)*1, ε_u(−0.50)*1	[15, 48]
Reinforcement ultimate tensile strength f_u [MPa]	*Lognormal*	$f_{u,exp}$	0.05	f_y (0.85)*1, ε_u(−0.55)*1	[48]
Reinforcement Young modulus E_s [MPa]	*Lognormal*	200000	0.03	-	[48]
Reinforcement ultimate strain ε_u [-]	*Lognormal*	0.09	0.09	f_y (−0.50)*1, f_u (−0.55)*1	[48]

* 1 (-) coefficient of linear correlation with respect to other material variables in agreement with [48].

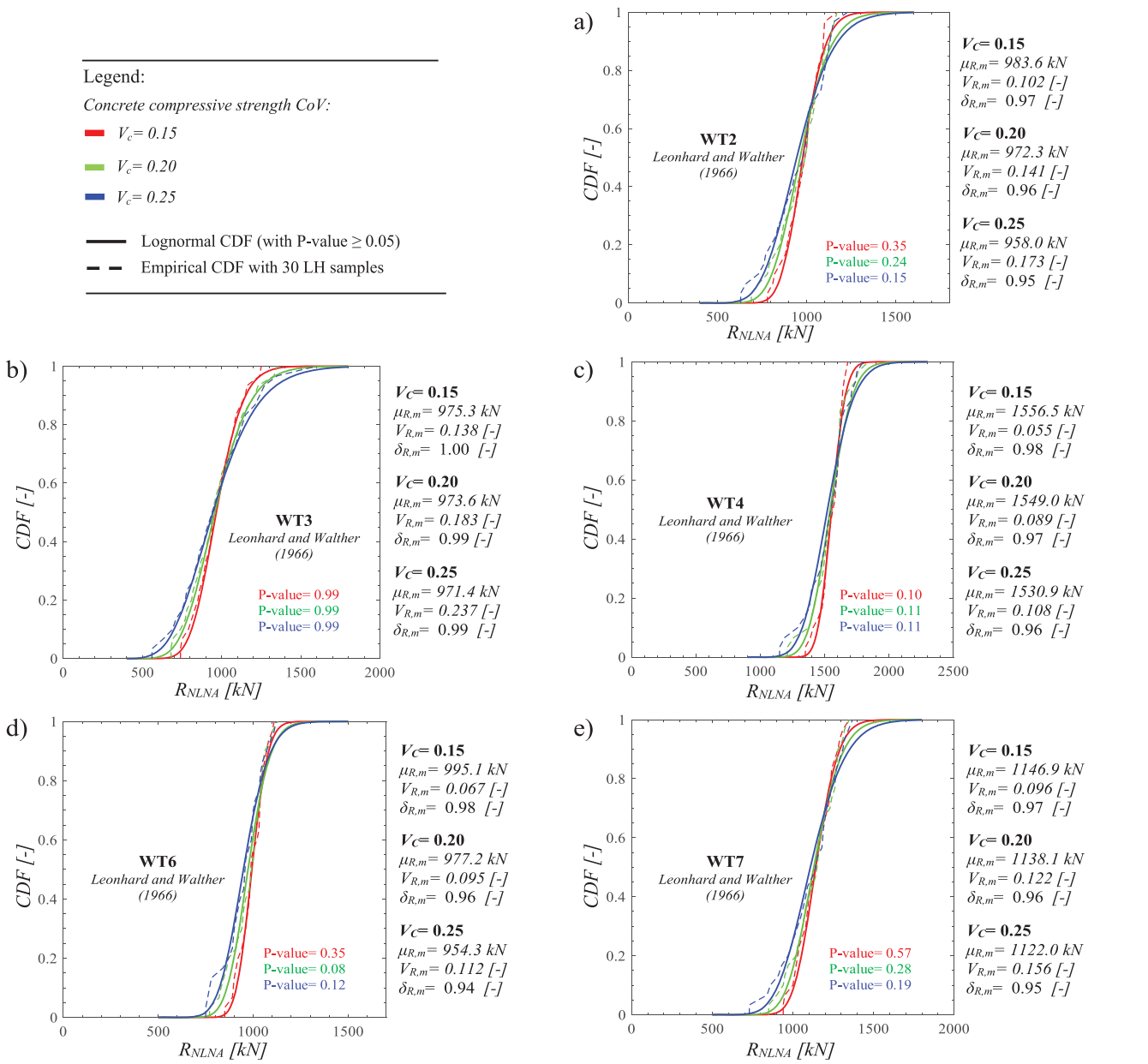

Fig. 9. Empirical and lognormal CDFs for the tests of [44].

achieve the best-fitting as well as the upper and lower bounds of the 95% confidence interval [59] of the fitting procedure.

Fig. 13(a)-(c) illustrate the value of $\delta_{R,m}$ with respect to the strain ratio $\varepsilon_{s,max}/\varepsilon_y$. The coefficients a and b according to Eq.(6) are related to the best-fit, upper and lower bounds of the 95% confidence interval, respectively, depending on the three assumptions regarding V_c (i.e., 0.15–0.20-0.25). The observed values related to the 16 RC members range between the values of 1.08 and 0.95. A slightly linear decreasing trend as a function of $\varepsilon_{s,max}/\varepsilon_y$ can be recognized in all the three assumptions on V_c with comparable values for the coefficients a and b. These results confirm the validity of the simplifying assumption frequently used in reliability analysis combined to the use of NLNAs [14,17,19]: the mean value of the probabilistic distribution of the global structural resistance $\mu_{R,m}$ aligns with the outcome of a single NLNA, assuming mean values for material properties and nominal values for geometrical properties (which, in this study, correspond to the experimental values f_{exp} and a_{exp}, respectively), denoted as $R_{NLNA}(f_m;a_n)$. Therefore, in practical applications, the value of the *mean-to-mean* deviation $\delta_{R,m}$ can be assumed, reasonably, equal to 1.

Fig. 14(a)-(c) depict the values of $V_{R,m}$ with respect to the strain ratio $\varepsilon_{s,max}/\varepsilon_y$. Similarly, the values of the coefficient η of Eq.(7) for the best-fit, upper and lower bounds of the 95% confidence interval related to η estimation are reported considering the three values for V_c. Comparable values of η are recognized for the different values of V_c. At very low values of $\varepsilon_{s,max}/\varepsilon_y$ (i.e., lower than 1), $V_{R,m}$ approaches the CoV assumed for the concrete cylinder compressive strength V_c, according to assumptions of Table 1. This behavior is related to a pure brittle failure mode of the RC system governed by the concrete compressive strength only without the yielding of the primary reinforcement in tension. As the ratio $\varepsilon_{s,max}/\varepsilon_y$ increases, it is evident that the value of $V_{R,m}$ progressively decreases with a non-linear trend as reflected by Eq.(7). When $\varepsilon_{s,max}/\varepsilon_y$ exceeds values between 5–10 (depending on the assumption of V_c), it approaches the CoV of the primary reinforcement yielding strength V_y, as specified in Table 1, indicating a failure mechanism primarily governed by the yielding of the main reinforcement. Notably, the function for $V_{R,m}$ is constrained between the values of V_c and V_y according to the

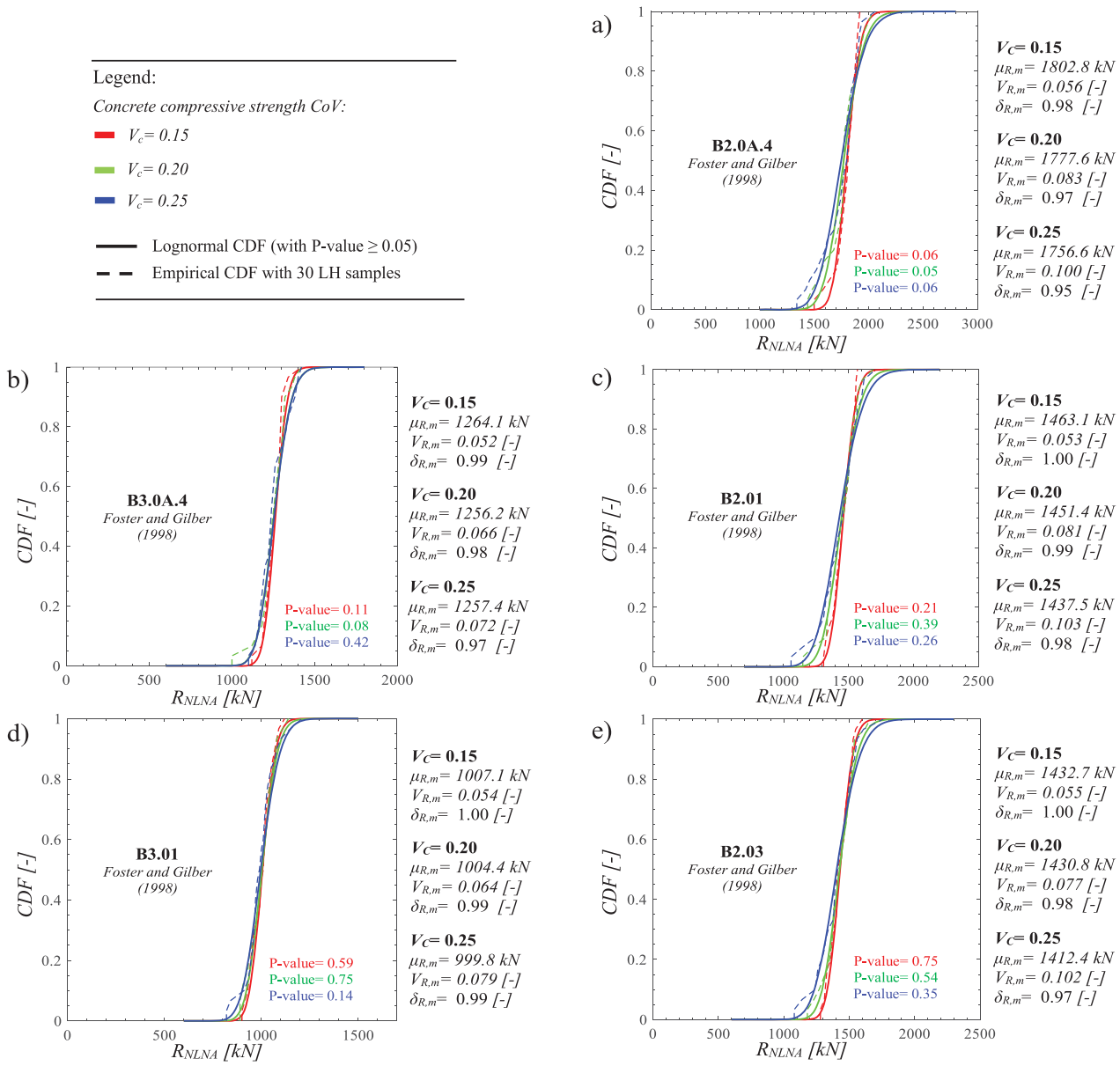

Fig. 10. Empirical and lognormal CDFs for the tests of [45].

probabilistic models outlined in Table 1.

In next section, the results so far presented are used to implement the proposed strain-based method according to the Global Resistance Method safety format within the GRF [15].

6. Evaluation of the global resistance safety factors by means of the strain-based method

In this section, the achievements of Section 5 are implemented to finalize the proposal of the strain-based method to assess the global resistance safety factor γ_R within the Global Resistance Method safety format according to the GRF [15]. First, the global resistance safety factors γ_R are calculated with reference to the different target reliability levels distinguishing between the different values of V_c. Finally, the predictions in terms of the design values of the global structural resistance R_d achieved by the novel approach are compared to ones of other safety formats within the GRF [15] (i.e., ECoV method and PFM [15]).

6.1. Proposals for practical applications of the strain-based method

The evaluation of the global resistance safety factor γ_R can be performed according to the philosophy of the GRF [15] through Eq.s(2)-(4). According to the GRM [15], the design value of the global structural resistance R_d can be derived through Eq.(1) adopting the results of one NLNA performed with mean and nominal values for materials f_m and geometrical properties a_n, respectively, as representative values. According to Eq.(2), the value of γ_R can be derived once one knows:

- the CoV of the global structural resistance V_R and the related bias factor δ_R;
- the target value of the reliability index β_t and the related FORM factor α_R [15,22].

To implement Eq.(2), it is essential to thoroughly examine Eq.s(3)-(4). In detail, Eq.(4) is used to calculate the CoV of the global structural resistance, V_R. It takes as input the values of the CoV of the global resistance related to the aleatory uncertainty of materials, $V_{R,m}$, and

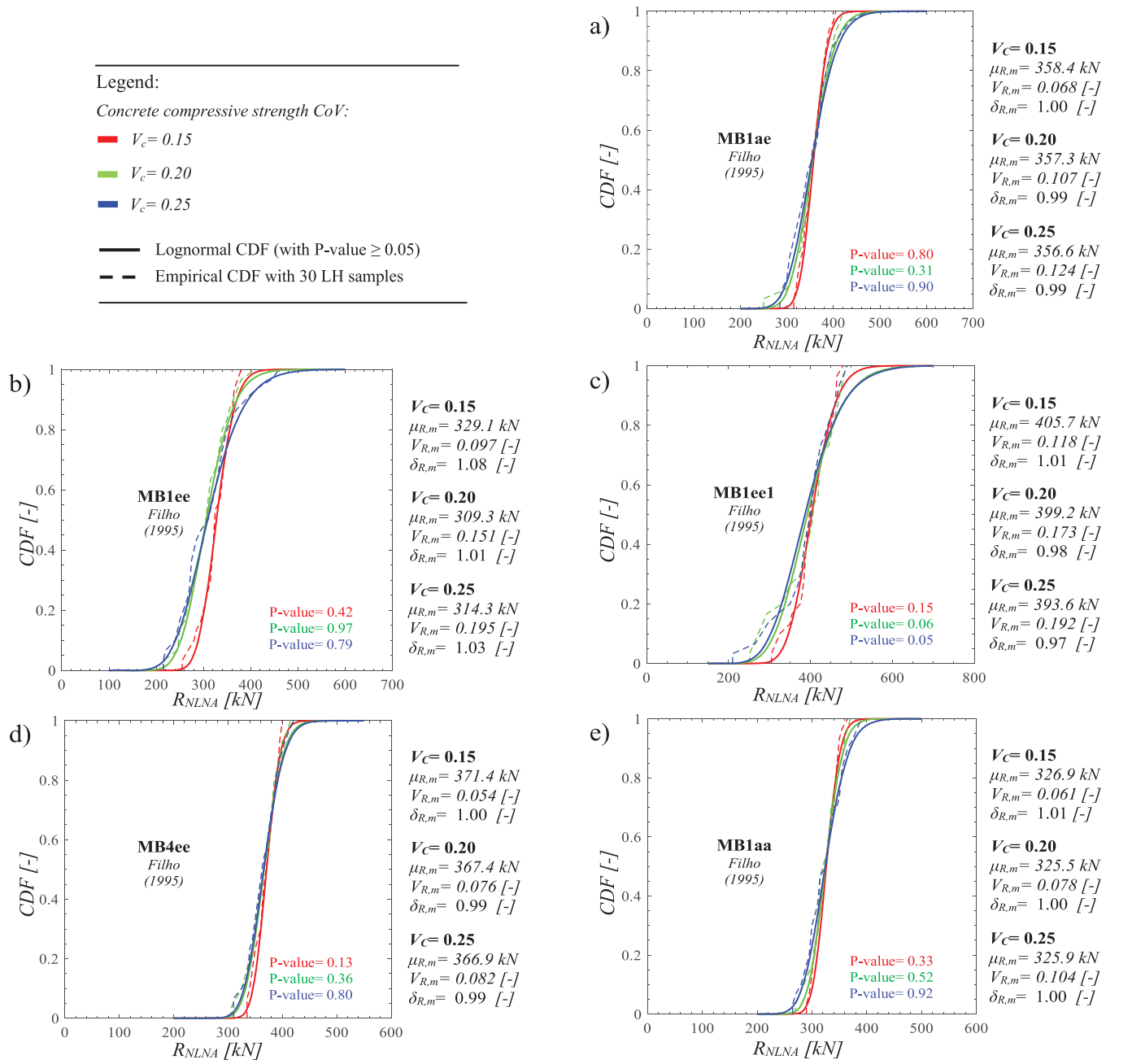

Fig. 11. Empirical and lognormal CDFs for the tests of [46].

geometry, $V_{R,g}$. As previously discussed in Section 2, the value of $V_{R,g}$ can be set equal to a constant value of 0.05 for non-slender RC members.

Regarding the value of $V_{R,m}$, it is proposed to adopt Eq.(7) assuming − 0.4 as coefficient η which is the average value between the three exponents corresponding to the lower bound values of the 95% confidence intervals in the estimation of η for the three V_c assumptions. As the value of the exponent η is negative, its lower bounds lead to the higher curves depicted in Fig. 14(b)-(c). This choice is driven by the need to consider statistical uncertainties for practical purposes. The peak strain attained in the primary reinforcement $\varepsilon_{s,max}$ derives from a single NLNA conducted with mean and nominal values for materials and geometrical properties, respectively. The so far established approach to estimate $V_{R,m}$ leads to the results reported in Fig. 15(a). Furthermore, the findings in Section 5, which illustrate the low sensitivity of the coefficient η to the chosen V_c value, suggest that Eq.(7), with $\eta = -0.4$, can potentially be applied to various V_c values as shown in Fig. 15(a). However, Eq.s(1)-(4) can be used to determine γ_R and R_d for V_R values lower than 0.30, as typically observed in RC structures and achieved in Section 5. For higher values (quite rare also in existing RC structures [49–52]), Eq.s(1)-(4) should be adapted according to [61] in the assumption of lognormal probabilistic distribution.

As far as the bias factor δ_R, its value can be determined by using Eq. (3) and depends on the values of $\delta_{R,m}$ and $\delta_{R,g}$. As discussed before, the value of $\delta_{R,g}$ can be set reasonably equal to 1.00 also in line with [14] and similarly, according to Section 4, $\delta_{R,m}$ can be also approximated as 1.00. For instance, a reasonable simplification for practical purposes can be to set the value of δ_R equal to 1.00 with the aim to derive the global resistance safety factor γ_R using Eq.(2).

Fig. 15(b)-(d) illustrate the results in terms of the global resistance safety factor γ_R determined according to Eq.(2) for V_c equal to 0.15 (b), 0.20 (c) and 0.25 (d) adopting some frequently used values as target reliability index β_t: 2.8 and 3.3 for existing RC structures with a

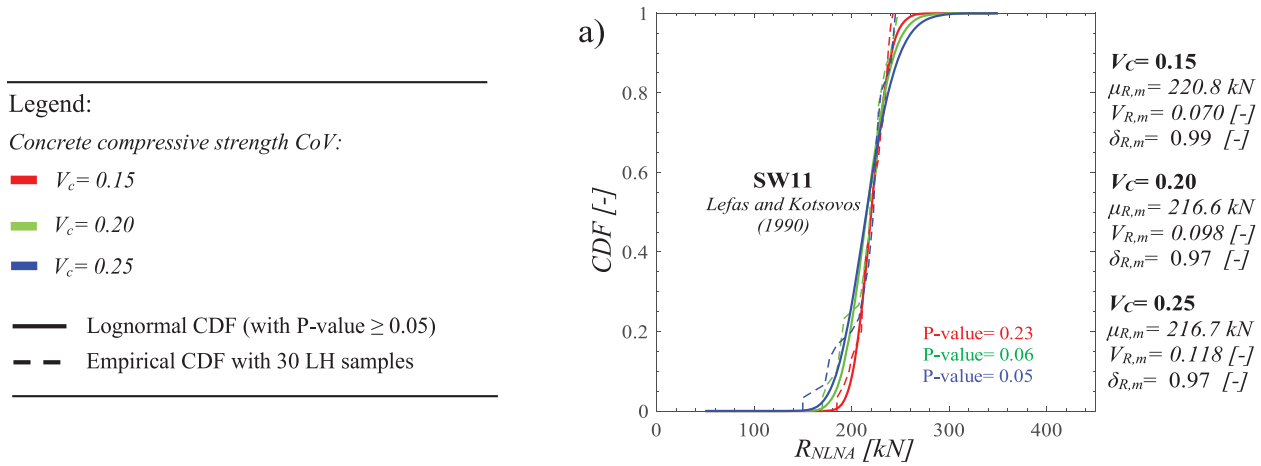

Fig. 12. Empirical and lognormal CDFs for the tests of [47].

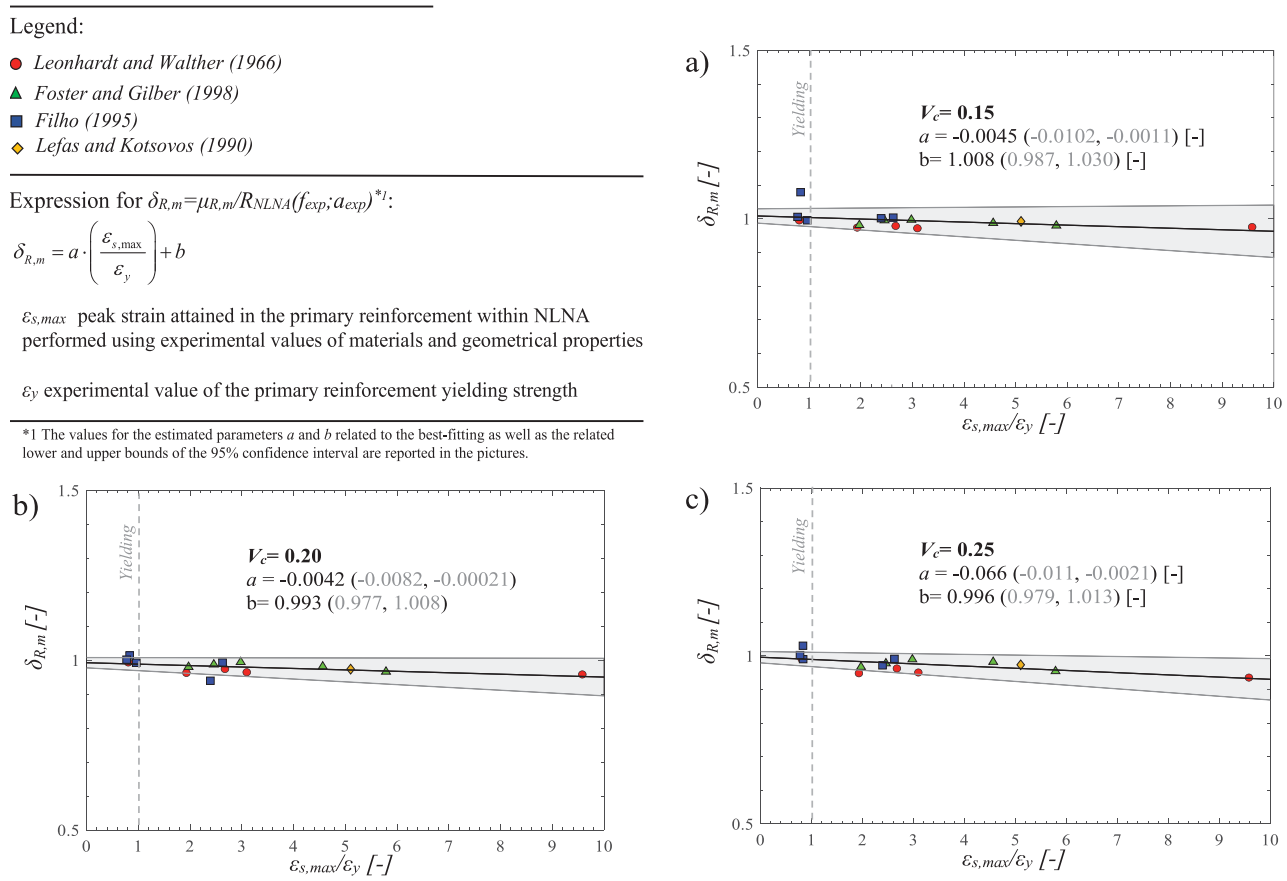

Fig. 13. Trend of variation of the *mean-to-mean* deviation $\delta_{R,m}$ with respect to the strain ratio $\varepsilon_{s,max}/\varepsilon_y$ concerning to the different assumptions for V_c (i.e., (a) 0.15, (b) 0.20, (c) 0.25). The values of a and b corresponding to the lower and upper bounds of the 95% confidence interval as well as the best-fit expression are, respectively, also reported.

reference working life different from 50 years [22]; 3.8 and 4.3 for new RC structures having 50 and 100 years as reference working life [15].

Note that Fig. 15(b),(c),(d) plot γ_R under the assumption of aleatory uncertainties (i.e., materials $V_{R,m}$ and geometry $V_{R,g}$) dominating with respect to epistemic (i.e., modeling hypotheses V_θ) ones, as per [15]. If the latter assumption is not verified considering explicitly the mechanical and geometrical uncertainties in addition to the "between" and "within" epistemic uncertainties, similar curves can be derived using the appropriate value of the first-order reliability method sensitivity factor α_R related to the non-dominant random variable. In this scenario, the model uncertainty would have a dominant influence on the reliability assessment of the structural system.

The proposed approach leads to the assessment of the global resistance safety factor γ_R for both new and existing RC structures accounting for appropriate target reliability level with the need to perform just one NLNA with mean values for material properties and nominal values for geometrical ones. With reference to the existing RC structures, the latter ones can be directly derived from testing and inspections [22].

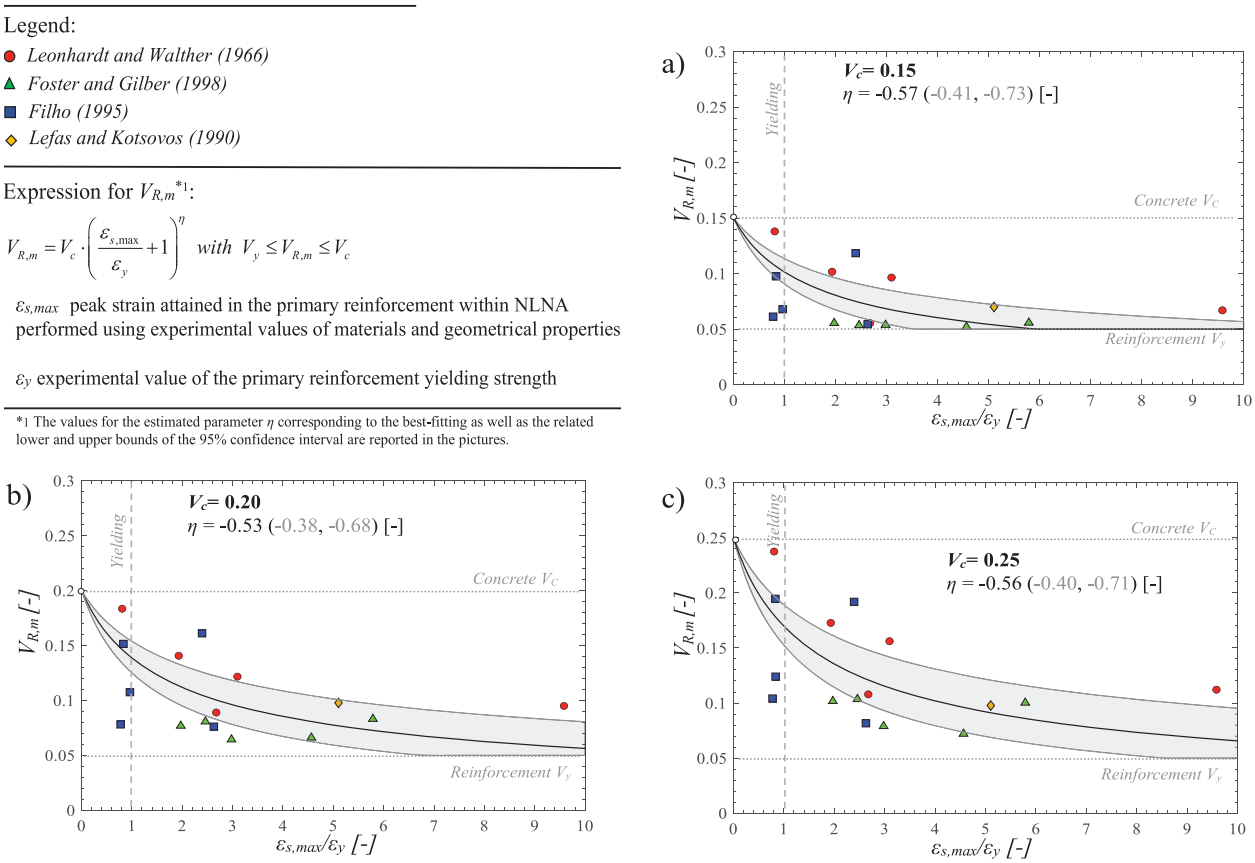

Fig. 14. Trend of variation of the CoV of the global resistance $V_{R,m}$ with respect to the strain ratio $\varepsilon_{s,max}/\varepsilon_y$ concerning to the different assumptions for V_c (i.e., (a) 0.15, (b) 0.20, (c) 0.25). The values of η corresponding to the lower and upper bounds of the 95% confidence interval as well as of the best-fit expression are, respectively, also reported.

Moreover, the method can easily account for the nature of the most likely failure mode that is affected by the reinforcement arrangement [62].

6.2. Comparison with other safety formats within the GRF

In this subsection, the comparison between the novel strain-based approach and other commonly used safety formats within the GRF is discussed for a value of β_t equal to 3.8 that is related to structures of new realization and reference working life of 50 years [15]. Specifically, the Estimation of Coefficient of Variation - ECoV method [15] and the Partial Factor Method - PFM [15] are considered.

These methods are applied following the guidelines of [15], as explained in Section 2, with adjustments made to account for the different values of the CoV for the concrete cylinder compressive strength, V_c [22]. The comparison is performed comparing the design value of the global structural resistance defined within each safety format R_d and the design value of the global structural resistance derived from the probabilistic analysis $R_{d,Prob}$ in the assumption of lognormally distributed random variable [14]. The value of $R_{d,Prob}$ has been determined considering both model and aleatory uncertainties [63] in agreement with the assumptions adopted for the three safety formats herein compared. Note that R_d was computed according to Eq.(1) with the additional factor 1.15 for all the safety formats in case the "non-decreasing assumption" [30,31] is not satisfied, as explained in Section 2.

For all the safety formats under consideration, the model uncertainty has been considered according to [38–43]. In detail, for simplicity without affecting the comparison, the value of γ_{Rd} has been set equal to 1.15 with reference to β_t equal to 3.8 under the assumption of non-dominant variable as suggested by [38] considering different solution strategies. Note that a specific distinction of the values of γ_{Rd} as a function of the failure mode characteristics can be performed when other solution strategies are adopted since it is possible to address the proper sensitivity factors regarding both aleatory and epistemic uncertainties. Additionally, materials and geometrical uncertainties have been considered in accordance with the information provided in the previous sections. The comparison is presented in Fig. 16 in terms of the ratio $R_d/R_{d,Prob}$ differentiating between the three values of V_c. The safety formats are on the safe side if they provide an adequate safety margin with the mean value of the ratio $R_d/R_{d,Prob}$ lower than 1.00. Fig. 16 shows that the mentioned above criterion is fulfilled for the proposed strain-based method, ECoV method and PFM. It can also be recognized that, in general, the scattering (i.e., CoV) of the estimates of $R_d/R_{d,Prob}$ is smaller for the novel strain-based method if compared to the ECoV and PFM. This demonstrates the effectiveness of the approach proposed for general applications as well as of the ECoV and PFM safety formats with the advantage to carry out just one NLNA with mean values of material properties and nominal values for geometrical characteristics.

7. Conclusions

This investigation has proposed a novel strain-based method to account for the influence of aleatory uncertainties related to material properties on the global structural response (i.e., CoV $V_{R,m}$) and estimate the design value of the global structural resistance using NLNAs in accordance with the Global Resistance Format (GRF). To achieve this, 16 RC members, experimentally tested by various authors, have been considered and accurately reproduced using appropriate non-linear modeling assumptions (i.e, solution strategies). Upon comparing the

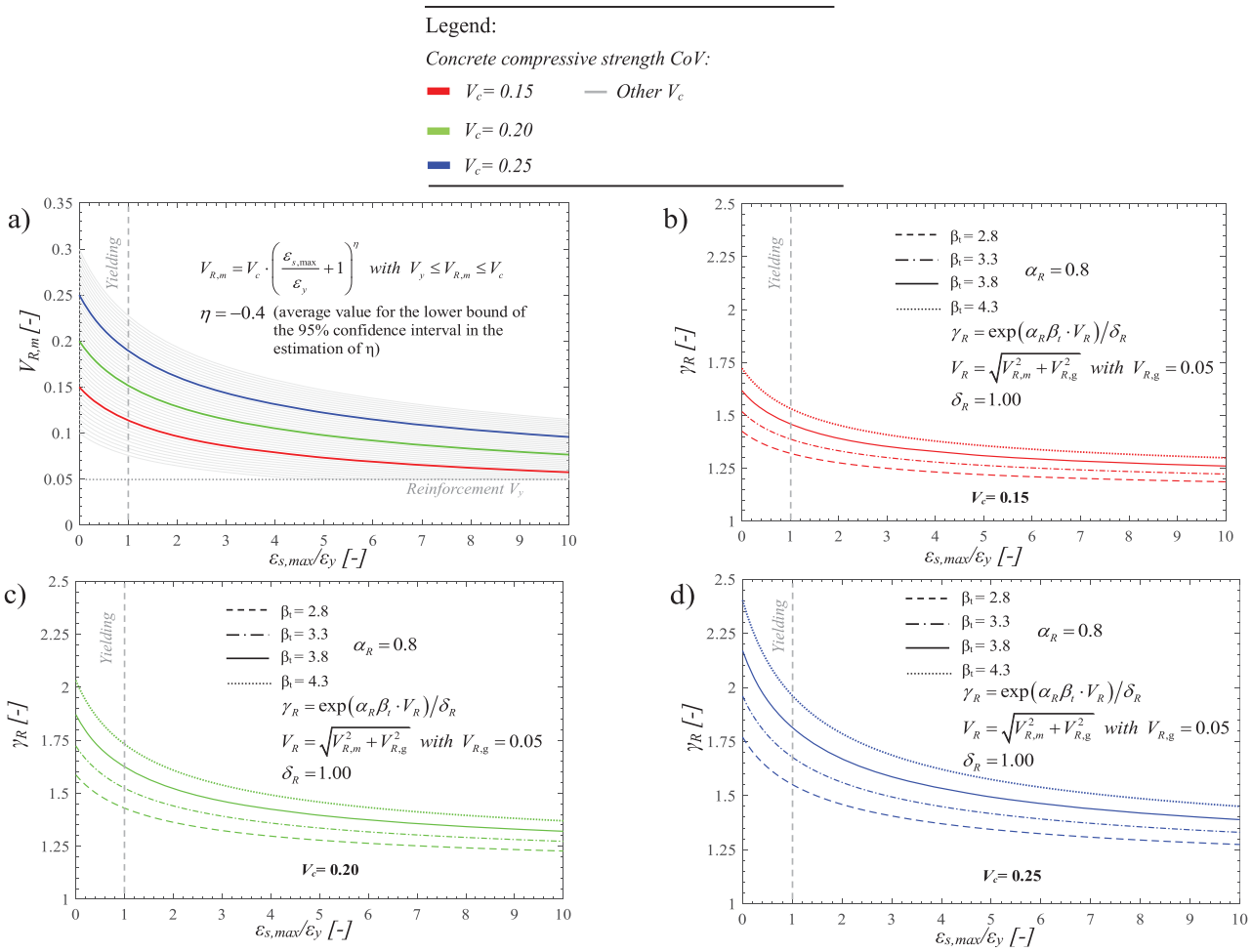

Fig. 15. Representation of the expressions of Eq.(7) evaluated adopting $\eta = -0.4$ for different values of V_c (a); evaluation of the global resistance safety factors for different target reliability indices β_t with respect to V_c: 0.15 (b), 0.20 (c) and 0.25 (d).

results with the experimental data, the model uncertainty associated with the chosen solution strategies has been quantified, effectively demonstrating their validity. Next, the 16 NLN models have been employed to conduct a probabilistic analysis of the global structural resistance, accounting for the aleatory uncertainty in materials. The primary objectives have been to characterize the mean value ($\mu_{R,m}$) and the CoV ($V_{R,m}$). The influence of concrete quality has been accounted for by incorporating three different assumptions for its CoV, V_c (0.15, 0.20, 0.25), into the probabilistic modeling.

Then, the correlation between $V_{R,m}$ and the ratio of the peak strain in the primary reinforcement ($\varepsilon_{s,max}$) over the reinforcement yielding strain (ε_y) is also proposed. Importantly, this ratio derives from the NLNA conducted with mean and nominal values for materials and geometrical properties, respectively, and provides insight into the structural response including information about the most likely structural failure mode. The best-fitting relationship and the expressions related to the lower and upper bounds of the 95% confidence interval have been derived. The adoption of the expression corresponding to the average lower bound of the 95% confidence interval related to the exponent η, set equal to − 0.4, has led to the definition of a suitable predictive relationship for estimating $V_{R,m}$. Subsequently, the global resistance safety factors (γ_R) have been determined as well as the design values of the global structural resistance in alignment with the GRM accounting for appropriate target reliability levels (for both new and existing structures). It is worth highlighting that just one NLNA is needed by using the mean and nominal values for materials and geometrical properties, respectively. This approach surely reduces the computational demand within the process related to the adoption of NLNAs for safety verifications in addition to avoid potential errors by the analyst. Moreover, it is open to possible applications with structural health monitoring systems in combination with the use of NLNAs for the reliability assessment of existing RC structures and infrastructures. Finally, the predictions of the proposed strain-based method have been compared with those of other safety formats within the GRF, such as the ECoV method and the PFM, thereby demonstrating the effectiveness of the research proposals. In conclusion, based on the several experimental tests and associated structural responses for the calibration of the novel strain-based method, the proposed approach can be employed for verifications of complex no slender RC structural members involving the use of NLNAs through the FE method. Further studies on other structures with respect to different failure modes (e.g., punching shear verifications in slabs without shear reinforcement) are necessary.

CRediT authorship contribution statement

Gino Diego: Writing – review & editing, Writing – original draft, Validation, Methodology, Investigation, Formal analysis, Data curation, Conceptualization. **Miceli Elena:** Writing – review & editing, Writing – original draft, Validation, Methodology, Investigation, Formal analysis, Data curation, Conceptualization. **Castaldo Paolo:** Writing – original draft, Validation, Supervision, Methodology, Investigation, Formal analysis, Conceptualization. **Recupero Antonino:** Supervision, Methodology, Investigation, Formal analysis, Conceptualization. **Mancini Giuseppe:** Supervision, Methodology, Investigation, Formal analysis,

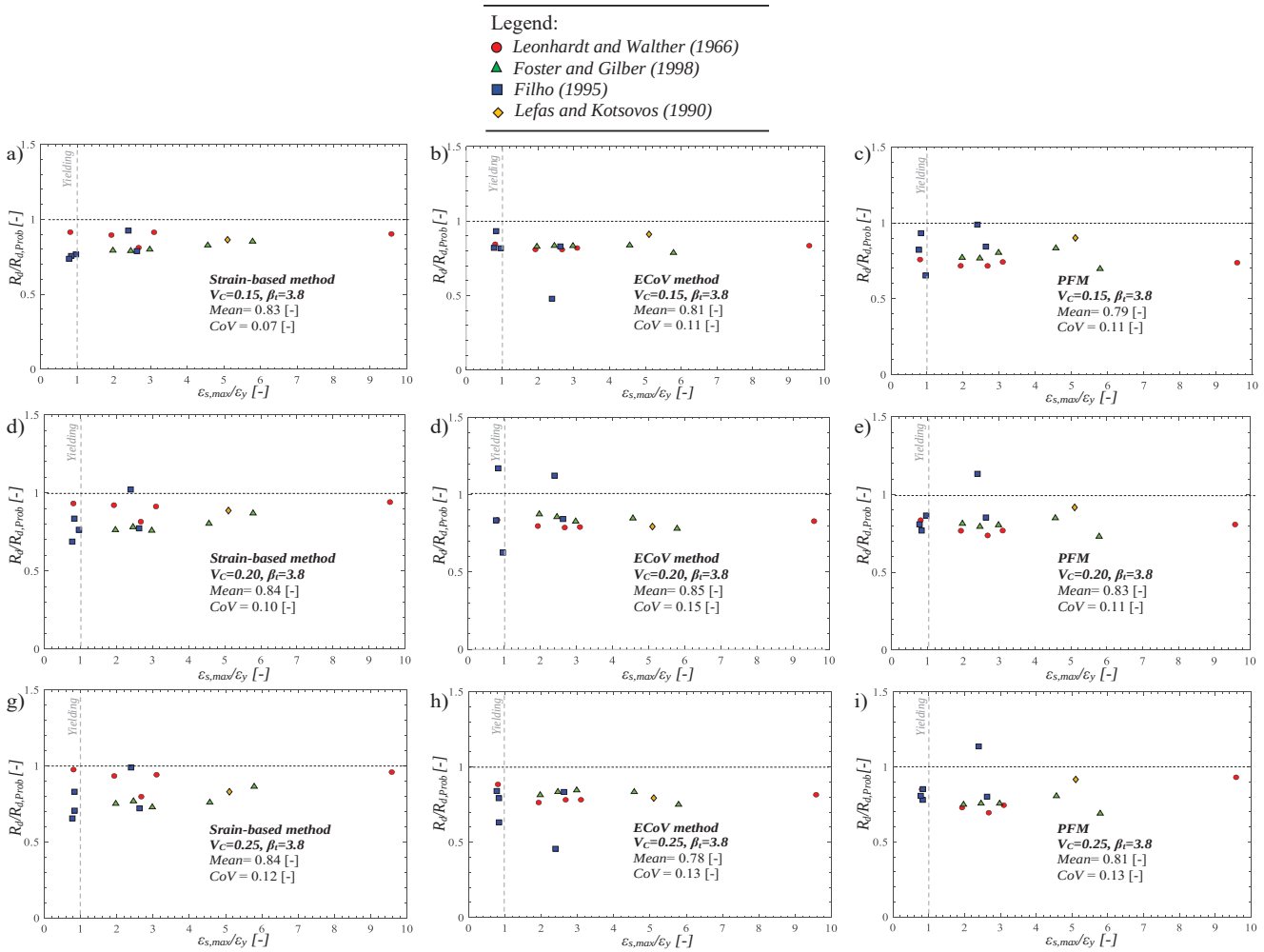

Fig. 16. Comparison between the strain-based method, ECoV method [15] and PFM [15], in terms of ratio between the estimated design value of the structural resistance R_d and the actual design global resistance from the probabilistic analysis $R_{,Prob}$.

Conceptualization.

Declaration of Competing Interest

No conflict of interest.

Data availability

Data will be made available on request.

Acknowledgments

This study was carried out within the *Ministerial Decree no. 1062/2021* and received funding from the *FSE REACT-EU - PON Ricerca e Innovazione 2014–2020*. This manuscript reflects only the authors' views and opinions, neither the European Union nor the European Commission can be considered responsible for them.

This work is part of the collaborative activity developed by the authors within the Commission 3 – Task Group 3.1: *"Reliability and safety evaluation: full-probabilistic and semi-probabilistic methods for existing structures"* of the International Federation for Structural Concrete (*fib*).

This work is also part of the collaborative activity developed by the authors within the framework of the *WP 11 – Task 11.4 – ReLUIS*.

This work is also part of the collaborative activity developed by the authors within the research project PRIN 2018–2021 "*Life-long optimized structural assessment and proactive maintenance with pervasive sensing techniques*".

This study was also carried out within the "*Data fusion based digital twins for structural safety assessment*" project – funded by European Union – Next Generation EU within the PRIN 2022 program (D.D. 104 - 02/02/2022 Ministero dell'Università e della Ricerca). This manuscript reflects only the authors' views and opinions and the Ministry cannot be considered responsible for them.

Annex A

This "Annex A" reports the results in terms of load vs displacement curves achieved from the probabilistic investigation of Section 5 with reference to the 16 RC members of [44–47] and differentiating between the three assumptions of the CoV for the concrete cylinder compressive strength (i.e., V_c = 0.15, 0.20, 0.25).

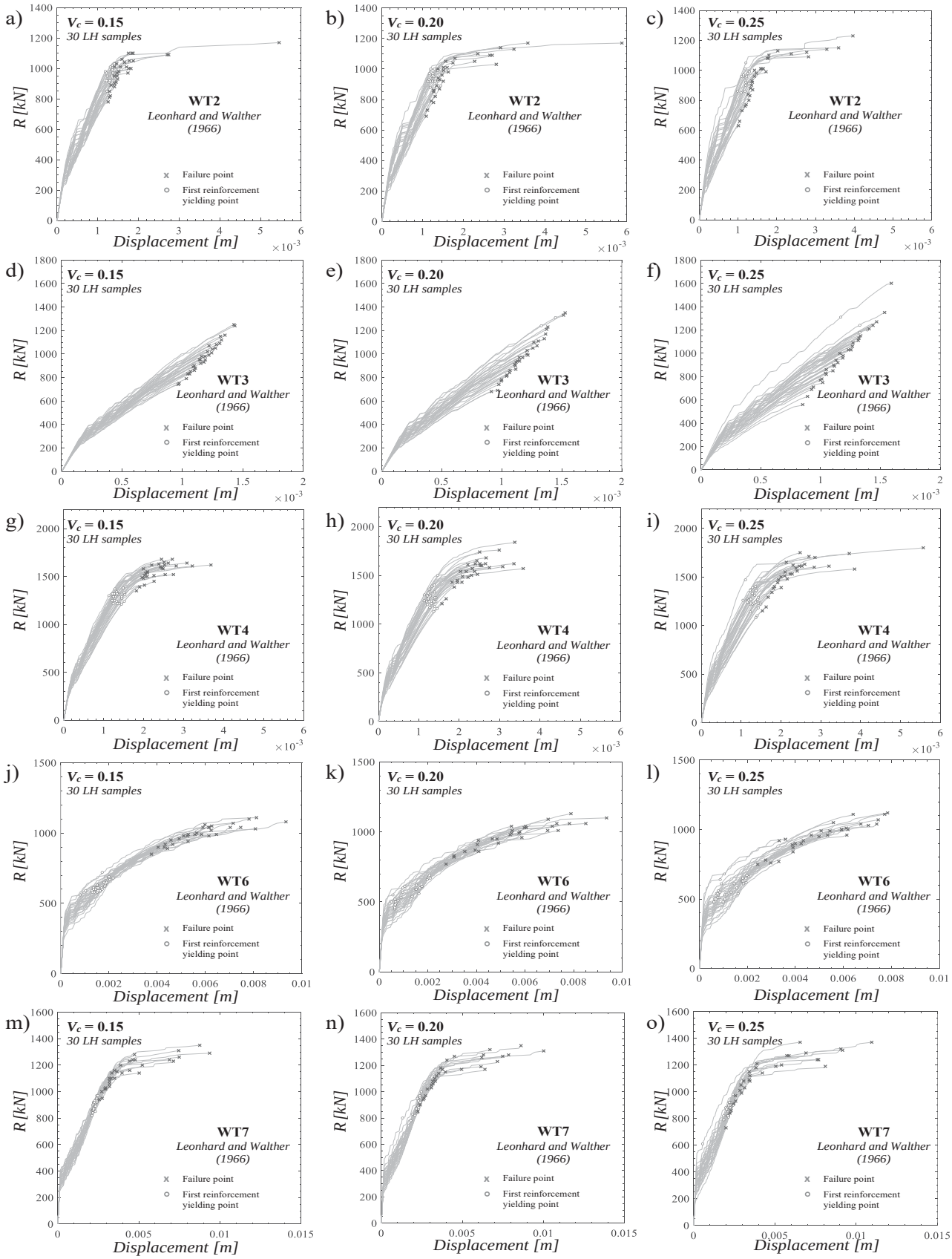

Fig. A1. Results in terms of load vs displacement from the probabilistic analysis of the RC members of [44].

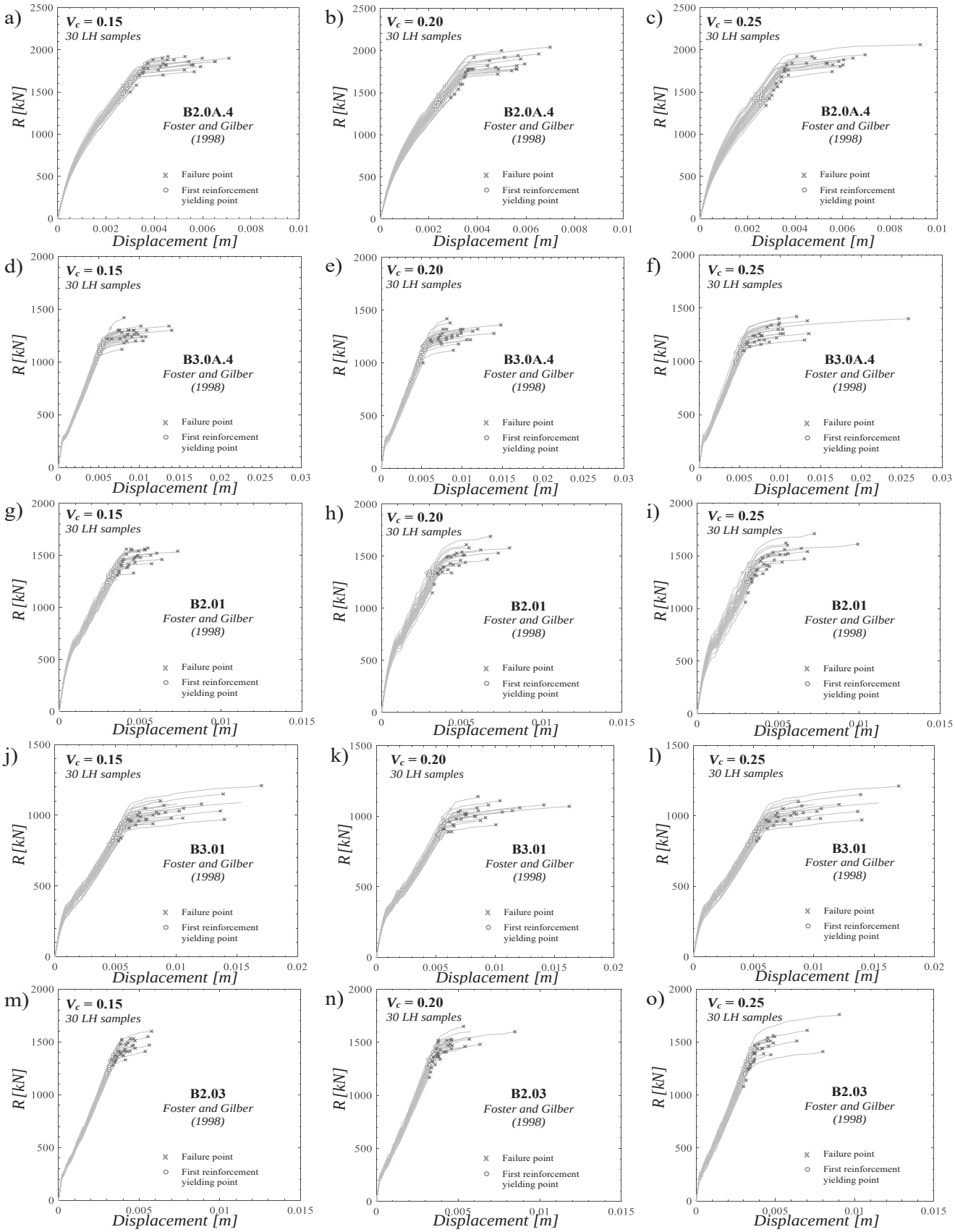

Fig. A2. Results in terms of load vs displacement from the probabilistic analysis of the RC members of [45].

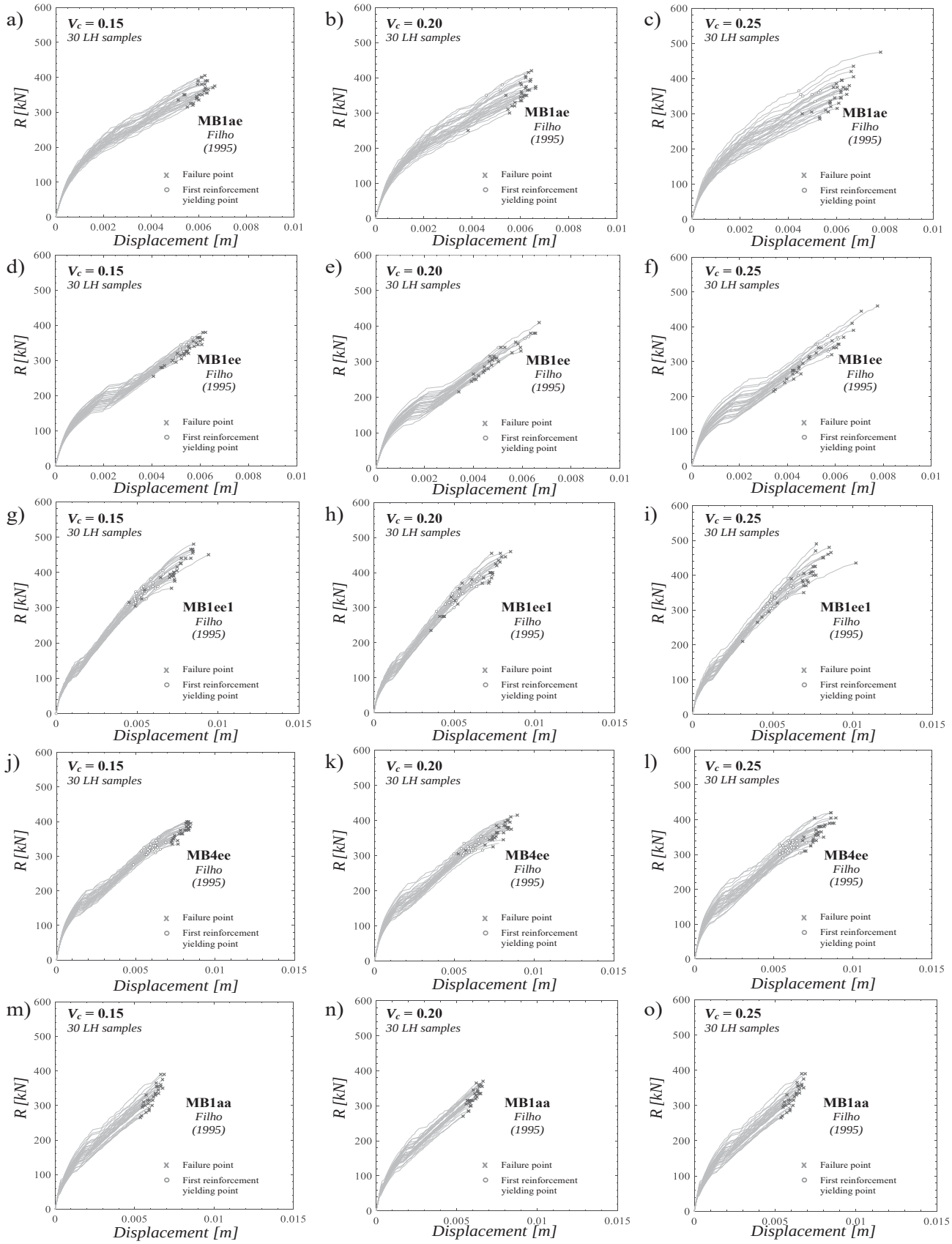

Fig. A3. Results in terms of load vs displacement for from probabilistic analysis of the RC members of [46].

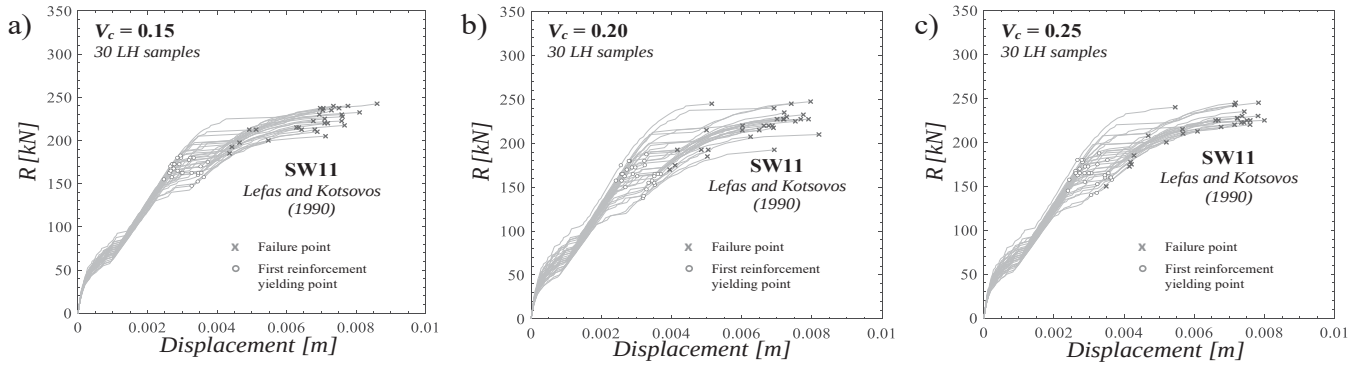

Fig. A4. Results in terms of load vs displacement from the probabilistic analysis of the RC members of [47].

References

[1] Abdel-Rahman AM, El-Din AS, El-Gawad HA. A review of nonlinear finite element analysis methods for reinforced concrete structures. Structures 2021;28:102034.
[2] Dashti F, Dhakal RP, Pampanin S. A parametric investigation on applicability of the curved shell finite element model to nonlinear response prediction of planar RC walls. 1 December Bull Earthq Eng 2019;Volume 17(Issue 12):6515–46.
[3] Dudziak S. Numerically efficient three-dimensional model for non-linear finite element analysis of reinforced concrete structures. Materials 2021;14:1578.
[4] Bagge N. Demonstration and examination of a procedure for successively improved structural assessment of concrete bridges. Struct Concr 2019:1–24.
[5] Rasulo A, Pelle A, Lavorato D, Fiorentino G, Nuti C, Briseghella B. Finite element analysis of reinforced concrete bridge piers including a flexure-shear interaction model. Appl Sci 2020;10(7):2209.
[6] Engen M, Hendriks MAN, Øverli JA, Åldtstedt E. Solution strategy for non-linear finite element analyses of large reinforced concrete structures. Str Concr 2015;(3):389–97.
[7] Most T. Assessment of structural simulation models by estimating uncertainties due to model selection and model simplification. Comput Struct 2011;89(17-18):1664–72.
[8] Blomfors M, Engen M, Plos M. Evaluation of safety formats for non-linear finite element analyses of statically indeterminate concrete structures subjected to different load paths. Struct Concr 2016;17(1):44–51.
[9] Pelle Angelo, et al. Time-dependent cyclic behavior of reinforced concrete bridge columns under chlorides-induced corrosion and rebars buckling. Struct Concr 2022;23(1):81–103.
[10] Belletti B., Scolari M., Vecchi F. PARC_CL 2.0 crack model for NLFEA of reinforced concrete structures under cyclic loadings. Computer and Structures 191: 165–179.
[11] Mohammed A, Almansour H, Martín-Pérez B. Simplified finite element model for evaluation of ultimate capacity of corrosion-damaged reinforced concrete beam-columns. Int J Adv Struct Eng 2018;10:381–400. https://doi.org/10.1007/s40091-018-0204-2.
[12] Slobbe A, Rózsás A, Allaix DL, Bigaj-van Vliet A. On the value of a reliability-based nonlinear finite element analysis approach in the assessment of concrete structures. Struct Concr 2019:1–16. https://doi.org/10.1002/suco.201800344.
[13] Di Sarno L, Pugliese F. Effects of mainshock-aftershock sequences on fragility analysis of RC buildings with ageing. ISSN 0141-0296 Eng Struct 2021;Volume 232:111837. https://doi.org/10.1016/j.engstruct.2020.111837.
[14] Castaldo P, Gino D, Marano GC, Mancini G. Aleatory uncertainties with global resistance safety factors for non-linear analyses of slender reinforced concrete columns. Eng Struct 2022;255:113920.
[15] *fib* Model Code for Concrete Structures; 2010. Fib 2013. Lausanne.
[16] Ftima MB, Massicotte B. Development of a reliability framework for the use of advanced nonlinear finite elements in the design of concrete structures. J Struct Eng 2012;138:1054–64.
[17] Allaix DL, Carbone VI, Mancini G. Global safety format for non-linear analysis of reinforced concrete structures. Struct Concr 2013;14(1):29–42.
[18] CEN. EN 1992–1-1: Eurocode 2 – Design of concrete structures. Part 1–1: general rules and rules for buildings. CEN; 2014. Brussels.
[19] Cervenka V. Reliability-based non-linear analysis according to fib model code 2010. Struct Concr 2013;14(1):19–28.
[20] Shlune H, Gylltoft K, Plos M. Safety format for non-linear analysis of concrete structures. Mag Concr Res 2012;64(7):563–74.
[21] prEN 1992–1-1:2021 Eurocode 2 – Design of concrete structures. Brussels.
[22] *fib* Bulletin N°80. Partial factor methods for existing concrete structures, Lausanne, Switzerland; 2016.
[23] Mourlas C, Markou G, Papadrakakis M. Accurate and computationally efficient nonlinear static and dynamic analysis of reinforced concrete structures considering damage factors. Eng Struct 2019;178:258–85.
[24] Li S, Coraddu A, Oneto L. Computationally aware estimation of ultimate strength reduction of stiffened panels caused by welding residual stress: from finite element to data-driven methods. Eng Struct 2022;264:114423.
[25] Permanoon A, Akhaveissy AH. Failure of existing structures with semi-brittle mechanical properties on meso scale and reduction of computational cost using non-linear topology optimization. Constr Build Mater 2022;Volume 319:126071.
[26] Mohsenian V, Nikkhoo A, Hajirasouliha I, Hejazi F. A low computational cost seismic analyses framework for 3D tunnel-form building structures. Adv Struct Eng 2022;25(14):2938–52. Doi:10.1177/13694332221113040.
[27] fib Bulletin N°45. Practitioner's guide to finite element modelling of reinforced concrete structures – State of the art report. Lausanne; 2008.
[28] DNV-RP-C208. Determination of structural capacity by non-linear FE analysis methods, Recommended Practice, DET NORSKE VERITAS AS; 2013, ⟨http://www.dnv.com⟩.
[29] Belletti B, Damoni C, Hendriks MAN. Development of guidelines for nonlinear finite element analyses of existing reinforced and prestressed beams. Eur J Environ Civ Eng 2011;15(9):1361–84.
[30] Castaldo P, Gino D, Mancini G. Safety formats for non-linear analysis of reinforced concrete structures: discussion, comparison and pr.oposals. Eng Struct 2019;193:136–53. https://doi.org/10.1016/j.engstruct.2018.09.041.
[31] Yua Q, Ruiz MF, Muttoni A. Considerations on the partial safety factor format for reinforced concrete structures accounting for multiple failure modes. Eng Struct 2022;264:114442.
[32] Malekloo A, Ozer E, AlHamaydeh M, Girolami M. Machine learning and structural health monitoring overview with emerging technology and high-dimensional data source highlights. Struct Health Monit 2022;21(4):1906–55. Doi:10.1177/14759217211036880.
[33] Singh T, Sehgal S, Prakash C, Dixit S. Real-time structural health monitoring and damage identification using frequency response functions along with finite element model updating technique. Sensors 2022;22:4546. https://doi.org/10.3390/s22124546.
[34] Jiménez Rios Alejandro, Plevris Vagelis, Nogal Maria. Bridge management through digital twin-based anomaly detection systems: a systematic review. Front Built Environ 2023;9. https://doi.org/10.3389/fbuil.2023.1176621.
[35] Liu Cheng, Zhang Peining, Xu Xuebing. Literature review of digital twin technologies for civil infrastructure. J Infrastruct Intell Resil 2023;2(3):100050. https://doi.org/10.1016/j.iintel.2023.100050.
[36] CEN. EN1990: Eurocode – Basis of structural design. CEN 2013. Brussels.
[37] Hasofer AM, Lind NC. Exact and invariant second moment code format. J Eng Div ASCE 1974;100(EM1):111–21.
[38] Castaldo P, Gino D, Bertagnoli G, Mancini G. Partial safety factor for resistance model uncertainties in 2D non-linear analysis of reinforced concrete structures. Eng Struct 2018;176:746–62. https://doi.org/10.1016/j.engstruct.2018.09.041.
[39] Engen M, Hendriks MAN, Köhler J, Øverli JA, Åldtstedt E. A quantification of modelling uncertainty for non-linear finite element analysis of large concrete structures. Struct Saf 2017;64:1–8.
[40] Kadlec L, Červenka V. Model uncertainties of FEM nonlinear analyses of concrete structures. Solid State Phenom 2016;249:197–202.
[41] Castaldo P, Gino D, Bertagnoli G, Mancini G. Resistance model uncertainty in non-linear finite element analyses of cyclically loaded reinforced concrete systems. Eng Struct 2020;211(2020):110496. https://doi.org/10.1016/j.engstruct.2020.110496.
[42] Gino D, Castaldo P, Giordano L, Mancini G. Model uncertainty in non-linear numerical analyses of slender reinforced concrete members. Struct Concr 2021.
[43] Engen M, Hendriks MAN, Monti G, Allaix DL. Treatment of modelling uncertainty of NLFEA in *fib* Model Code 2020. Struct Concr 2021;22:3202–12. https://doi.org/10.1002/suco.2021004203212ENGENETAL.
[44] Leonhardt F., Walther R. Wandartige Träger. Deutscher Ausschuss für Stahlbeton. Heft 178. Ernst & Sons. Berlin. Germany; 1966.
[45] Foster SJ, Gilbert J. Experimental studies on high strength concrete deep beams. Acids Struct J 1998;95:382–90.

[46] Filho J.B. Dimensionamento e comportamento do betao estrutural em zonas com discontinuitades. PhD thesis. Universidade Tecnica de Lisbona; 1995.
[47] Lefas ID, Kotsovos MD. Behaviour of reinforced concrete structural walls: strength, deformation characteristics and failure mechanism. Acids Struct J 1990;87:23–31.
[48] JCSS. JCSS Probabilistic Model Code. 2001.
[49] Pereira N, Romão X. Assessing concrete strength variability in existing structures based on the results of NDTs. Constr Build Mater 2018;173:786–800.
[50] Masi A, Digrisolo A, Santarsiero Giuseppe. Analysis of a large database of concrete core tests with emphasis on within-structure variability. Materials 2019;12:1985. https://doi.org/10.3390/ma12121985.
[51] Li, Ying, Vrouwenvelder, Ton Wijnants, Geert Henk. Spatial Variability of Concrete Degradation; 2003. 49–58. 10.1061/40707(240)6.
[52] Yang Yiming, Tang Huang, Wang Xinzhong. Failure probability analysis of corroded RC structures considering the effect of spatial variability. Mag Concr Res 2023;75(4):163–75. 2023.
[53] Olsson A, Sandberg G, Dahlblom O. On latin hypercube sampling for structural reliability analysis. Struct Saf 2003;25(1):47–68.
[54] ATENA 2D v5.9. *Cervenka Consulting s.r.o.*. Prague. Czech Republic; 2022.
[55] Saatcioglu Murat, Razvi Salim R. Strength and ductility of confined concrete. J Struct Eng 1992;118(6):1590–607.
[56] Holický M, Retief JV, Sikora M. Assessment of model uncertainties for structural resistance. Probabilistic Eng Mech 2016;45:188–97.
[57] Aly AB, El-Sherbiny MA, Abdel-Fattah MM, El-Rayes HH. Variation of steel reinforcement properties in RC structures: a review. Constr Build Mater 2022;279:124774.
[58] Hastie T, Tibshirani R, Friedman JH. The elements of statistical learning. 2nd ed..,. New York, NY: Springer; 2009.
[59] Faber Michael Havbro. Statistics and probability theory. Springer; 2012.
[60] Anderson TW, Darling DA. Asymptotic theory of certain "goodness-of-fit" criteria based on stochastic processes. Ann Math Stat 1952;23:193–212. https://doi.org/10.1214/aoms/1177729437.
[61] Taerwe RL. Toward a consistent treatment of model uncertainties in reliability formats for concrete structures. CEB Bull d'Information 1993;105-S17:5–34.
[62] Menichini Giovanni, Gusella Federico, Orlando Maurizio. Methods for evaluating the ultimate capacity of existing RC half-joints. Eng Struct 2024;Volume 299:117087. https://doi.org/10.1016/j.engstruct.2023.117087.
[63] Castaldo P, Gino D, Carbone VI, Mancini G. Framework for definition of design formulations from empirical and semi-empirical resistance models. Struct Concr 2018;19(4):980–7.